Drude Model of Electronic Conduction 1

Simplest model: electrons are accelerated by applied $\vec{E}$ and are colliding with scatterers. collisions are instantaneous processes when electrons change their $\vec{v}$. Thermalization occurs only during collisions, after collision $\vec{v}$ corresponds to T.

Current density: $\vec{J}_e = -ne\langle\vec{v}\rangle$ Drift velocity of e- gas: $m\vec{a} = \frac{d\vec{v}}{dt} = -e\vec{E} \Rightarrow \vec{v}(t) = -\frac{e\vec{E}}{m}t + \vec{v}(0)$

Collisions restore e- $\vec{v}$ to local thermal equilibrium. We label t as elapsed time before previous collision. Is velocity at t_0 will be v_0, and it will get some eE/m in between collisions. We assume random motion without contribution of v_0 to average electronic velocity.

Carrier mobility μ

Therefore: $\langle\vec{v}\rangle = -\frac{e\vec{E}}{m}\langle t\rangle = -\frac{e\tau}{m}\vec{E} \Rightarrow \vec{J} = \frac{ne^2\tau}{m}\vec{E} = \sigma\vec{E}$

Defining mean free path $l_e = \langle v\rangle\tau$ we get: $\sigma = \frac{ne^2\tau}{m} = \frac{ne^2 l_e}{m\langle v\rangle}$ and $\mu = \frac{e\tau}{m} = \frac{el_e}{m\langle v\rangle}$

Electron density: $n = N_A z\rho_m / A$

Mass density

Valence

Atomic weight

Drude Model of Electronic Conduction 2

In the absence of scattering $\tau \to \infty$ and therefore $\sigma \to \infty$. Real materials have defects, so there is always some residual scattering ~ τ_0 and σ_0. We can assume that scattering from phonons is independent process, therefore we can write: Matthiessen's rule

$$\rho = \frac{m}{ne^2}\left(\frac{1}{\tau_0} + \frac{1}{\tau_{ph}}\right)$$

Time dependent electric field: $\vec{E}(t) = \vec{E}(\omega)e^{-i\omega t} \Rightarrow \sigma(\omega) = \frac{(ne^2\tau)/m}{1 - i\omega\tau}$ σ_0

Also using Maxwell equations we get wave equation: $\nabla^2\vec{E} = -\frac{\omega^2}{c^2}\varepsilon(\omega)\vec{E}$

See derivation Aschroft-Mermin

Where: $\varepsilon(\omega) = 1 + \frac{4\pi i\sigma}{\omega}$

For $\omega\tau >> 1$ $\quad \varepsilon(\omega) = 1 - \frac{\omega_p^2}{\omega^2}; \omega_p^2 = \frac{4\pi ne^2}{m}$

→ for $\omega < \omega_p$ electric field decays exponentially in electron gas

→ for $\omega > \omega_p$ solutions are oscillatory and radiation can propagate

Electrical Conductivity and Fermi-Dirac Statistics

Occupation probability

$f_0=[\exp(\varepsilon(k)-\mu)+1]^{-1}$

$$\vec{j} = -\frac{e}{4\pi^3}\int_{k_{occ}} v(\vec{k})d\vec{k} = -\frac{e}{4\pi^3}\int_{1stBZ} v(\vec{k})f(\vec{k})d\vec{k}$$

due to scattering

Not $f_0(\mathbf{k})$ since this $f_0(\mathbf{k})$ is for equillibrium, with no T gradients and no external fields (eg. **E**). Real f=f(**r**,**k**) so that f(**r**,**k**)**drdk** is the number of e$^-$ in drdk (6D). Liouville theorem – phase space volume is conserved – so:

$$f(t+dt,\vec{r}+d\vec{r},\vec{k}+d\vec{k}) = f(t,\vec{r},\vec{k}) \Rightarrow f(t+dt,\vec{r}+d\vec{r},\vec{k}+d\vec{k}) - f(t,\vec{r},\vec{k}) = \left(\frac{\partial f}{\partial t}\right)_s dt$$

$$\dot{\vec{r}} = \vec{v}(\vec{k}); \hbar\dot{\vec{k}} = \vec{F}(\vec{r},\vec{k}) = -e(\vec{E}+\vec{v}\times\vec{B})$$

$\vec{B}$ → 0

$$\frac{\partial f}{\partial t} + v\nabla_r f + \frac{\vec{F}}{\hbar}\nabla_k f = \left(\frac{\partial f}{\partial t}\right)_s$$

Boltzmann transport equation

In steady state $\partial f/\partial t=0$ and $\nabla_r f = 0$

Using relaxation time approximation:

$$\left(\frac{\partial f}{\partial t}\right)_s \sim -\frac{\left|f(\vec{k})-f_0(\vec{k})\right|}{\tau(\vec{k})} \Rightarrow -\frac{e\vec{E}}{\hbar}\nabla_k f(\vec{k}) = -\frac{\left|f(\vec{k})-f_0(\vec{k})\right|}{\tau(\vec{k})} \Rightarrow f(\vec{k}) = f_0(\vec{k}) + \frac{e}{\hbar}\tau(\vec{k})\vec{E}\nabla_k f(\vec{k})$$

Surface element with constant E

We approximate here $\nabla_k f(\vec{k}) \sim \nabla_k f_0(\vec{k})$

$$\vec{j} \approx -\frac{e}{4\pi^3}\int v(\vec{k})\left[f_0(\vec{k}) + \frac{e}{\hbar}\tau(\vec{k})\vec{E}\nabla_k f_0(\vec{k})\right]d\vec{k}$$

$$d\vec{k} = dS_\varepsilon dk_\perp = dS_\varepsilon \frac{d\varepsilon}{|\nabla_k \varepsilon|} = dS_\varepsilon \frac{d\varepsilon}{\hbar v(\vec{k})}$$

conductivity σ_x

$$\Rightarrow j_x - \frac{e^2}{4\pi^3}\int v_x(\vec{k})\left[f_0(\vec{k}) + \frac{e}{\hbar}\tau(\vec{k})E_x\frac{\partial f_0}{\partial x}\right]d\vec{k} = -\frac{e^2E_x}{4\pi^3}\int v_x^2(\vec{k})\tau(\vec{k})\frac{\partial f_0}{\partial\varepsilon}d\vec{k}$$

$$\frac{df_0}{d\varepsilon} \approx -\delta(\varepsilon-\varepsilon_F)$$

Since integral for **k**=0 =0 due to inv. symmetry around k=0 in 1st BZ

Since $\partial f_0/\partial k_x = \hbar v_x(\partial f_0/\partial\varepsilon)$

Resistance and Resistivity in Experiment

Resistivity in Drude model:

$\sigma = ne^2\tau/m \qquad \rho = 1/\sigma$

$\rho(T)$ is determined by $\tau(T)$:
e^- - ph ($T>>\theta_D$) $1/\tau_{ph} \sim T \rightarrow \rho_{ph} \sim T$
e- - ph ($T<\theta_D$) $1/\tau_{ph} \sim T^3$ but $\rho_{ph} \sim T^5$ (Bloch-Grüneisen) due to small angle scattering e^- - e^- at low t $\rho \sim T^2$ (Fermi Liquid), or $\rho \sim T$ (non-Fermi liquid), etc…)
Therefore ρ(T,H) can tell us something about interactions – but – one has to note all (scattering) processes in order to be able to analyze the data.

Which gives us some basic insight into electronic transport in new material: n and / or τ

Another useful viewpoint:

$$\sigma \approx \frac{e^2}{4\pi^3\hbar}\int \frac{v_x^2(\vec{k})}{v(\vec{k})}\tau(\vec{k})\delta(\varepsilon-\varepsilon_F)dS_\varepsilon d\varepsilon = \frac{e^2}{4\pi^3\hbar}\int_{\varepsilon=\varepsilon_F} \frac{v_x^2(\vec{k})}{v(\vec{k})}\tau(\vec{k})dS_\varepsilon$$

Which tells us that electrical conductivity of a metal is a surface integral over the Fermi surface in ***k*** space – it is **proportional to the area of Fermi surface available for conduction**.

NOTE: the measured electrical resistivity will contain an impurity scattering term, ρ_0 which appears additively. This is often associated with chemical impurities as well as a variety of structural defects.

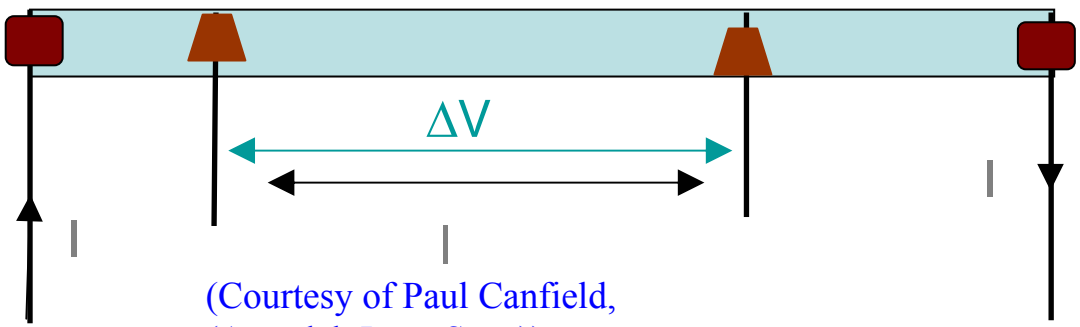

(Courtesy of Paul Canfield, (Ameslab Iowa State))

$R = \Delta V/I$

$R = \rho l/A$

Care in measuring DV, I, l and A is, of course, needed

Four Wire DC and AC Resistance Measurement

Two contacts are used to pass a current through the sample, two leads are used in order to measure the voltage drop. This configuration eliminates the resistance of the test leads from the measurement since voltage drop is measured directly on the sample, as opposed in the case of two probe measurement. A four-wire connection does not eliminate thermal EMF:

$$R = \frac{(V_1 + V_{th}) - (-V_1 + V_{th} + \delta V_{th})}{|2I|}$$

0 for fast switching, small T change

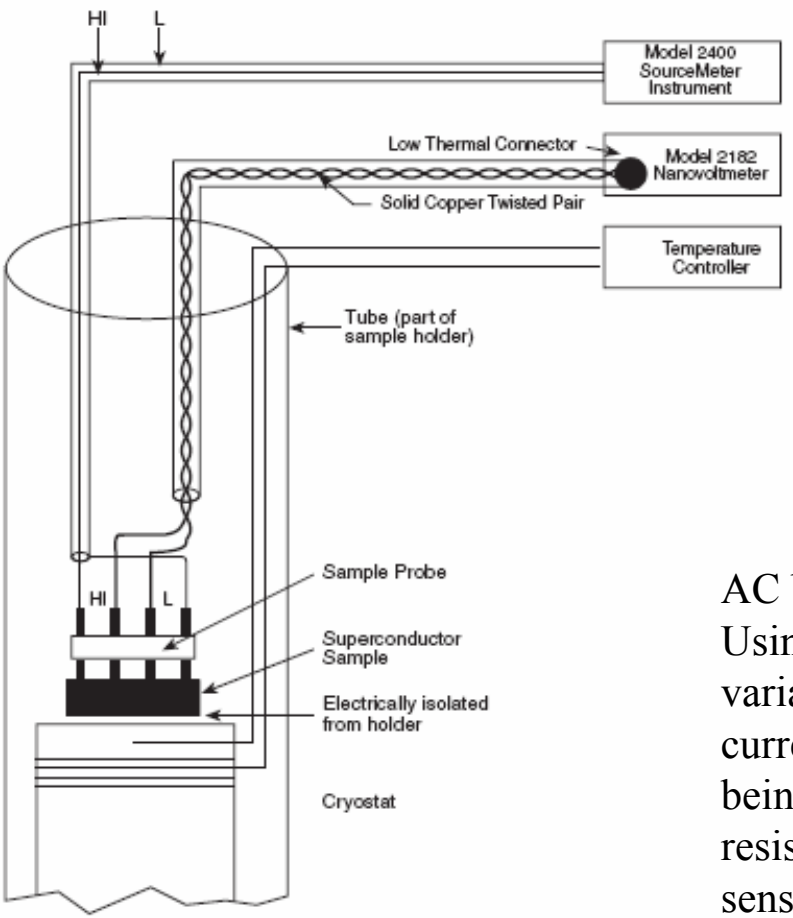

Current is applied to two adjacent leads using constant current source, and the voltage is measured across the other two leads using digital voltmeter.

The current was then reversed and the voltage measured again. The two values are subtracted, and the difference is divided by two, in order to cancel thermal voltages.

AC bridges use four-wire circuit where thermal EMFs are eliminated Using AC excitation current source. Excitation frequency is fixed or variable. Resistance is measured by passing the selected excitation current through an internal, high-stability reference resistor and sampl being measured. Excitation with constant current (small sample resistivity) or constant voltage is possible. It allows for use of sensitive lock in amplifiers with high noise rejection.

AC resistance Measurement

Wheatstone bridge not suitable for small resistances. Many bridges are used for thermometry ($10 - 10^3\ \Omega$, however for highly conductive single crystal samples at low T small noise is needed on signal level ~ $10^{-3}\ \Omega$.

The LR-700 AC Resistance Bridge uses a 4-wire AC measurement technique. A fixed magnitude AC sine wave current is applied to the sensor resistor through the I-Hi, I-Lo leads. The resulting voltage, returned by the V-Hi and V-Lo leads, is balanced against a known R-Set sine wave (and X-Set cosine wave) resulting in an analog difference signal ΔR and ΔX. The ΔR or ΔX analog signal is continuously sent to the analog temperature control circuitry to generate an analog heater output current. These signals are also available as ±10VDC analog output voltage at rear panel BNC connectors. Meanwhile, a microcontroller calculates values every 200 milliseconds and sends R-Set, ΔR, or R etc. to the display and/or as an output to the IEEE-488 or RS-232 digital interface. When controlling temperature, the temperature setpoint is controlled by R-Set (X-Set). The sensor temperature is indicated by R and the ΔR indicates the difference between the setpoint and sensor temperature. The R-Set sine waves originate in a programmable precision AC attenuator with digital management. This method delivers good linearity, resolution, and near zero AC offset.

The current generator uses reference resistors much greater than the sensor resistance. Johnson noise of the room temperature reference resistor is therefore greatly attenuated when delivered to the sensor by the LR-700 current generator. This technique is superior to wheatstone bridge type circuitry where the sensor is driven by a resistor whose value is comparable to the sensor resistance value.

More on bridges for low noise sample measurement: Physica Scripta 14, 257 (1986)

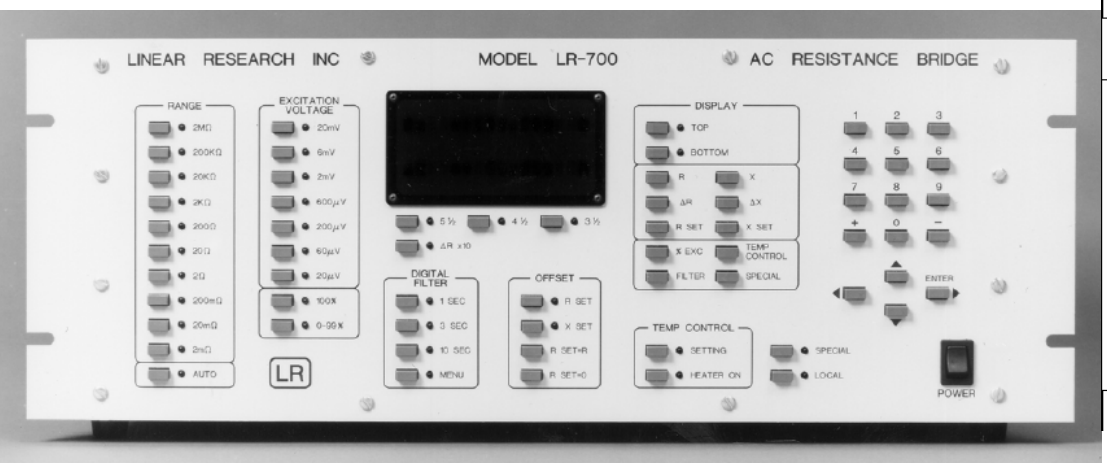

SENSOR EXCITATION CURRENT TABLE

		100% EXCITATION VOLTAGE, RMS								
		2μV †	6μV †	20μV	60μV	200μV	600μV	2mV	6mV	20mV
RANGE	2mΩ	1ma	3ma	10ma	30ma	LR-710	LR-710	X	X	X
	20mΩ	100μa	300μa	1ma	3ma	10ma	30ma	LR-710	LR-710	X
	200mΩ	10μa	30μa	100μa	300μa	1ma	3ma	10ma	30ma	LR-710
	2Ω	1μa	3μa	10μa	30μa	100μa	300μa	1ma	3ma	10ma
	20Ω	100na	300na	1μa	3μa	10μa	30μa	100μa	300μa	1ma
	200Ω	10na	30na	100na	300na	1μa	3μa	10μa	30μa	100μa
	2KΩ	1na	3na	10na	30na	100na	300na	1μa	3μa	10μa
	20KΩ	0.1na	0.3na	1na	3na	10na	30na	100na	300na	1μa
	200KΩ	LR-740	LR-740	0.1na †	0.3na †	1na	3na	10na	30na	100na
	2MΩ	LR-740	LR-740	LR-740	LR-740	0.1na †	0.3na †	1na	3na	10na

Notes: For any particular range and excitation voltage selected, the actual value of excitation voltage appearing across the sensor resistor is directly proportional to the magnitude in ohms of the sensor resistor. † indicates use of variable excitation.

Van der Pauw Method for Resistivity

Sample with thickness d << width and length (plate – like), with no holes. Four ohmic contacts on the sample << dimensions of the sample.

$$\left(e^{-\frac{\pi d R_{AB,CD}}{\rho}} + e^{-\frac{\pi d R_{BC,DA}}{\rho}} \right) = 1$$

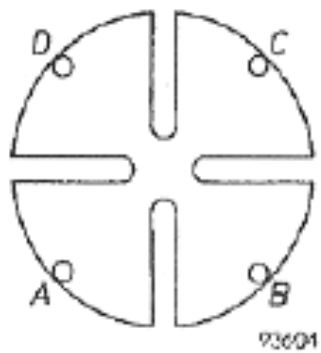

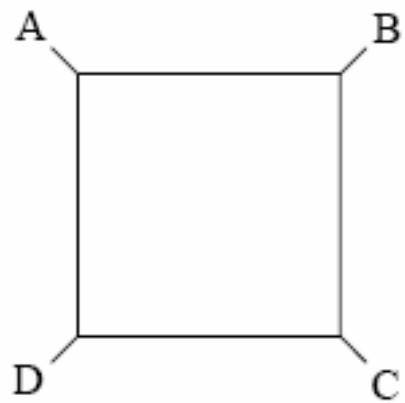

Where $R_{AB,CD} = (V_D - V_C)/I_{AB}$

$R_{BC,DA} = (V_A - V_D)/I_{BC}$

Preferred and possible sample geometry

In practice rarely used with single crystal samples since in most cases it is easier to fabricate needle – like sample

Philips Res. Repts. 13, 1 (1958)
Philips Res. Repts. 20, 220 (1958)

Crystal Sample Preparation for Resistivity 1

As opposed to heat capacity or to some extent magnetization measurement, electrical transport is easily influenced by extrinsic effects (flux from crystal growth, oxide layer,….)

Sample geometry is obtained using high resolution optical microscope

$$\rho = \frac{V \bullet A}{I \bullet l} = R\frac{A}{l}$$

In polycrystalline samples measuring sample geometry DOES NOT allow determination of ρ due to grain boundaries

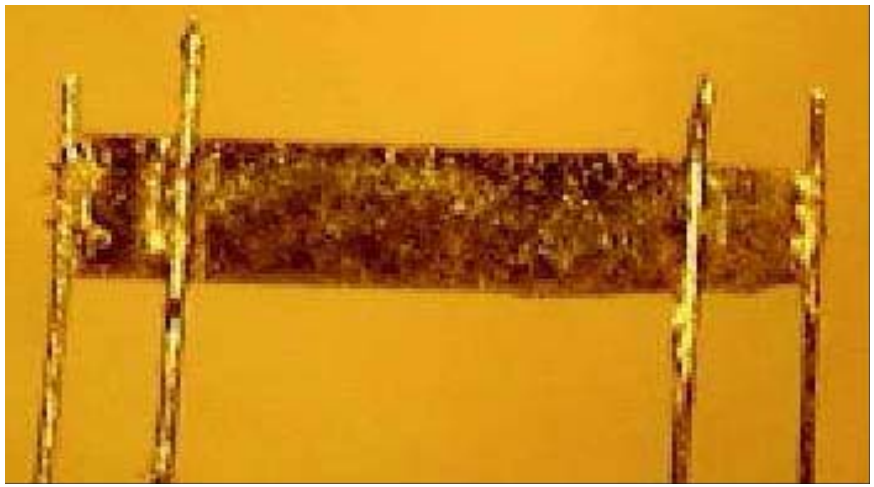

Note that in exp. we measure R= ρl/A, Therefore to increase signal/noise ratio, it is good to have long thin samples, especially for highly conductive metals at low T.

$CeCoIn_5$ four wire resistivity sample for dillution refrigerator measurement. A typical prepared sample size of >>1 mm, 0.2x0.1 mm results in typical sample resistances of < 10 mΩ at low temperatures. Soldering the Ag wires to samples using pure Indium results in contact resistance of ~ 5 mΩ at low T (courtesy of Johnpierre Paglione, UMD)

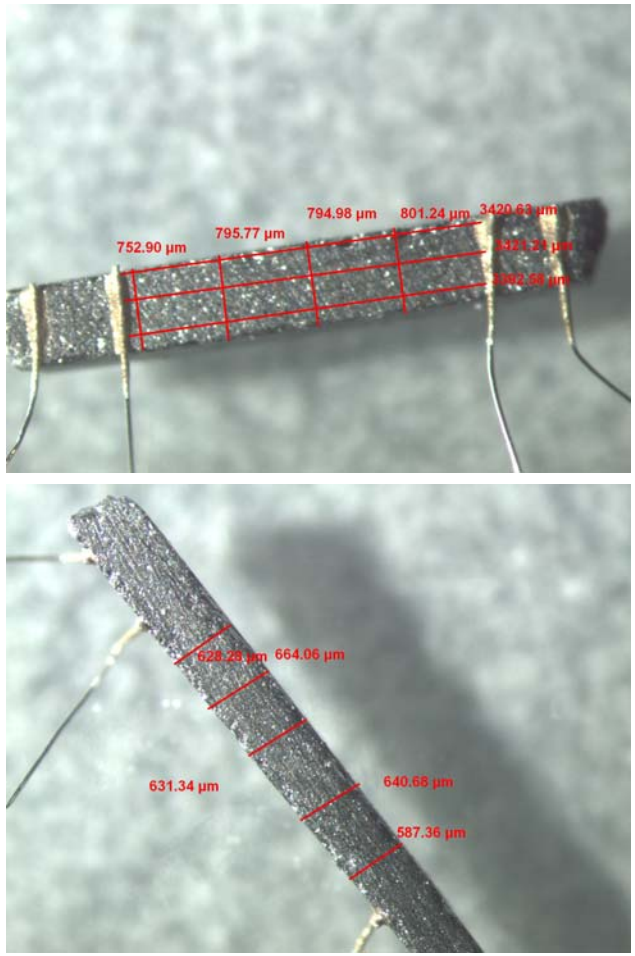

Four wire resistivity samples - Petrovic lab BNL

Crystal Sample Preparation for Resistivity 2

Flux grown crystals are often easy to prepare, particularly if they have thin needle or plate morphology.

Sometimes, particularly if crystal is grown using other methods, one has to mechanically separate, cut and polish crystals into appropriate geometry since long separation between voltage leads is desirable when measuring low resistances (low T, good conductivity).

Flux grown crystals have often to be etched in acid to remove excess flux that can cause extrinsic effects.

A highly conductive contact between sample and probe wire is required to minimize self-heating effects in low-T resistivity measurements ($P=I^2R$ in DC measurement, but also frequency dependence for AC measurement),

Most often employed contact methods are:

1. Epo-Tek H20E Ag epoxy cured at T= 100- 150ºC
2. Silver or carbon paint (dries at room T)
3. Gold evaporation of contacts (requires evaporator)
4. Soldering pure metals (In, Ga..)
5. Soldering metal eutectics:

There is no "best" contact method, some are better at He3 and He4 temperatures, some are stronger, some react with sample..

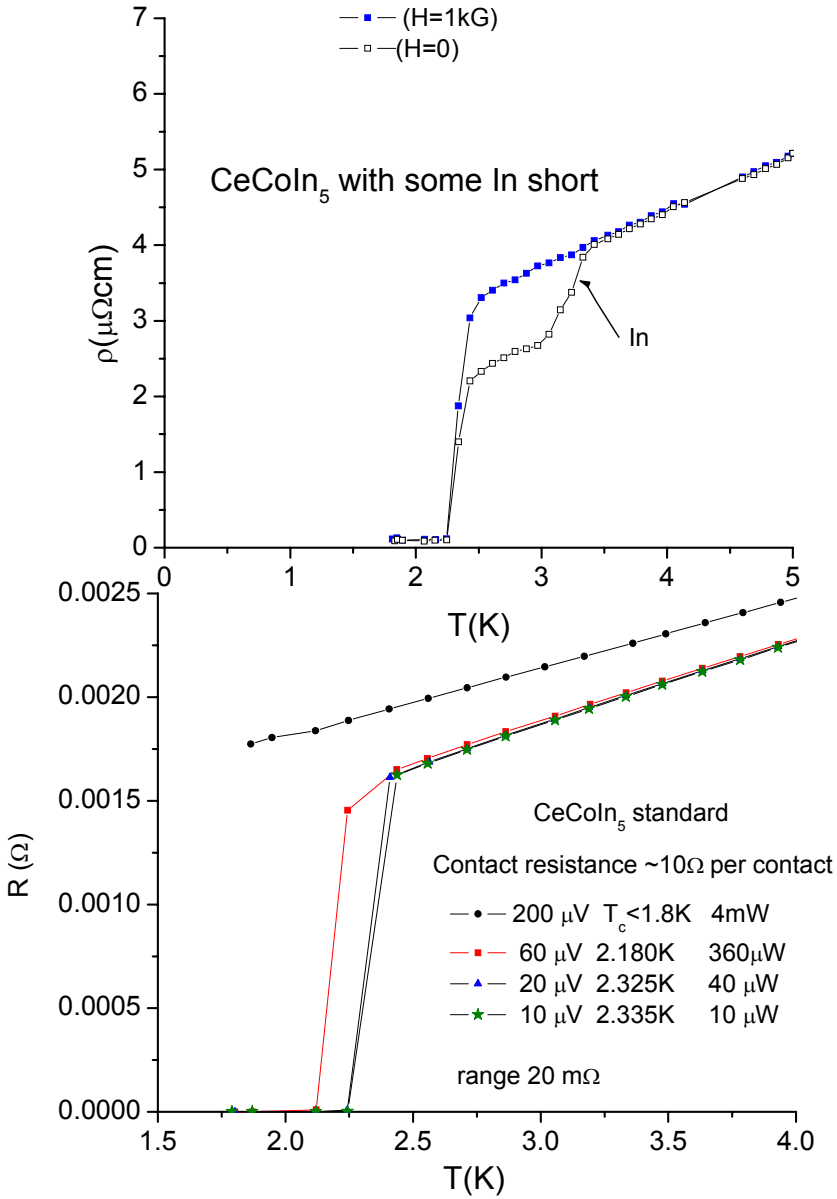

Residual Resistivity Ratio

For a simple metal the resistivity can often be modeled by:

$\rho = f(T) + \rho_0$ $f(T) \sim AT^2$ at lowest T

and $f(T) \sim BT$ at intermediate T

ρ_0 reflects finite nature mean free path. In materials synthesis ρ0 can be a measure of crystalline order, however other effects may increase ρ0 (hybridization in heavy fermion systems, various magnetic scattering, etc…

The residual resistivity ratio: RRR, is a measure of how defect free (or defected) a metallic sample is.

RRR = ρ(high T) /ρ(low T)

Often RRR = ρ(300 K)/ρ(2 K or 4.2K)

NOTE: RRR is also R(HT)/R(LT) since factors of l/A cancel out.

High RRR means low ρ_0.

J. Magn. Magn. Mater. 261, 210 (2003)

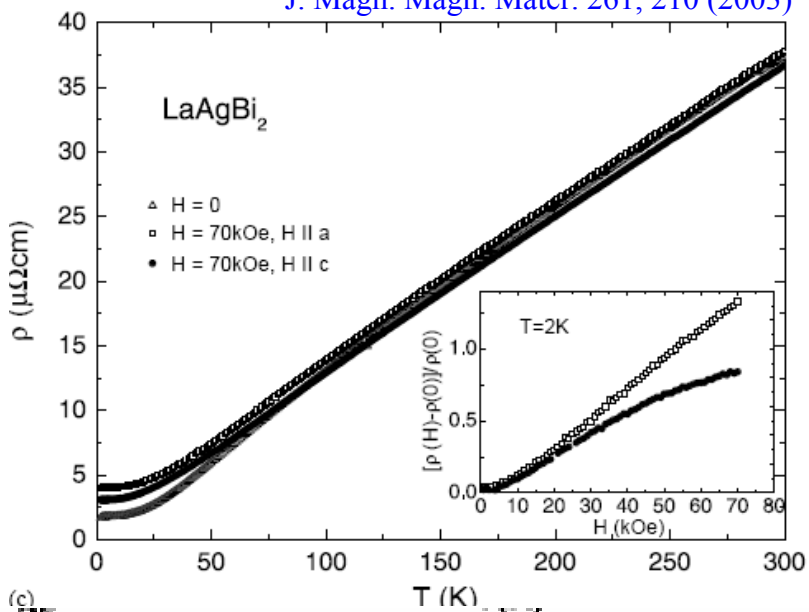

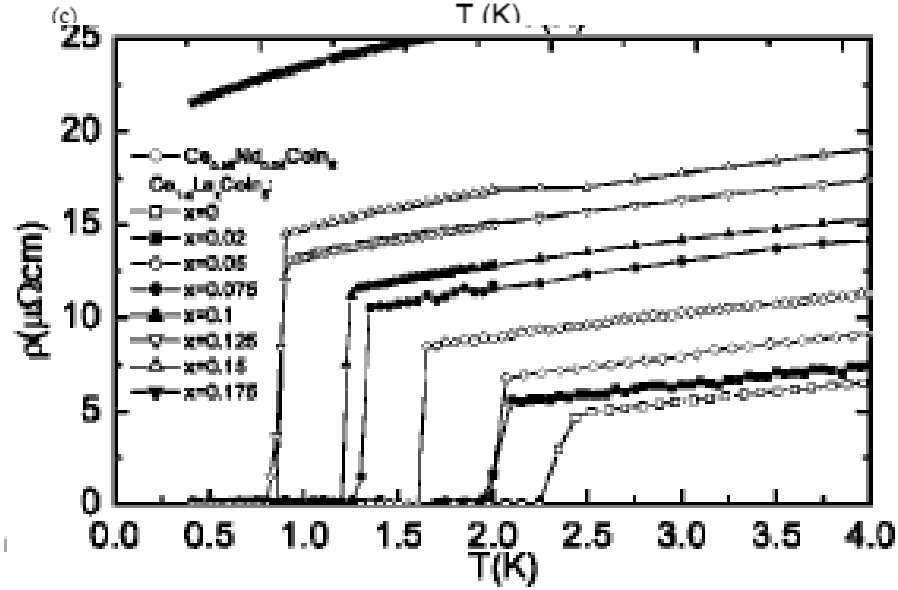

Phys. Rev. B 66, 054534

Control and Influence of Synthesis Parameters

Influence of synthesis parameters on materials quality Can be estimated using measurement of R and ρ.

In this case influence of Mg stoichiometry, B purity were investigated.

In addition, it was shown that large RRR is direct consequence of sample quality and not extrinsic effect.

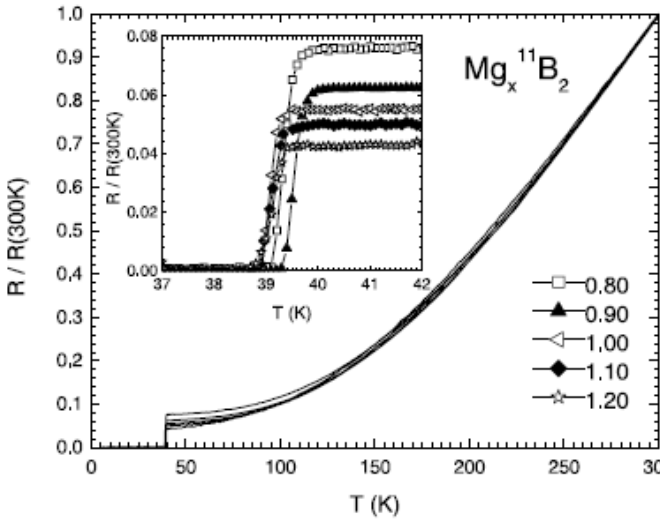

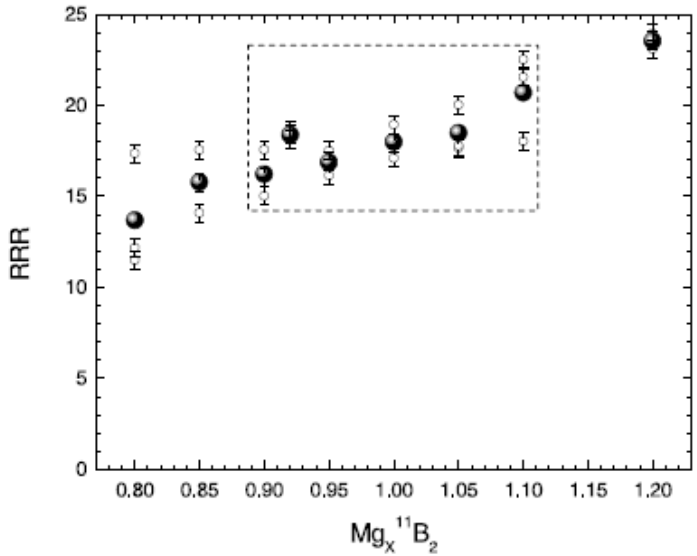

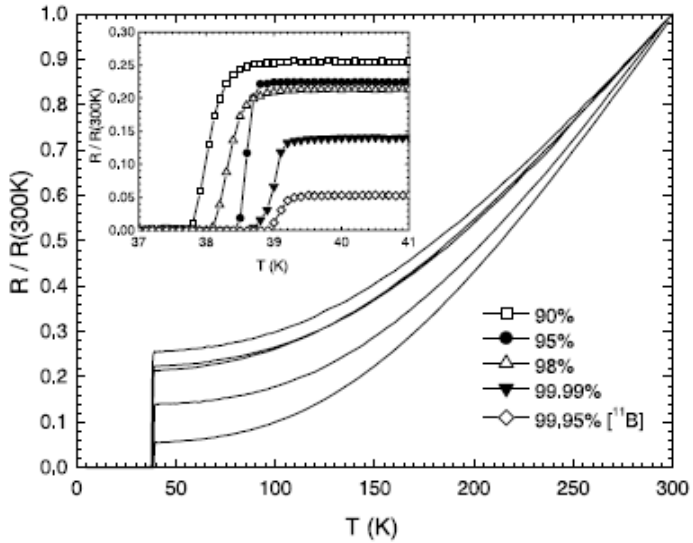

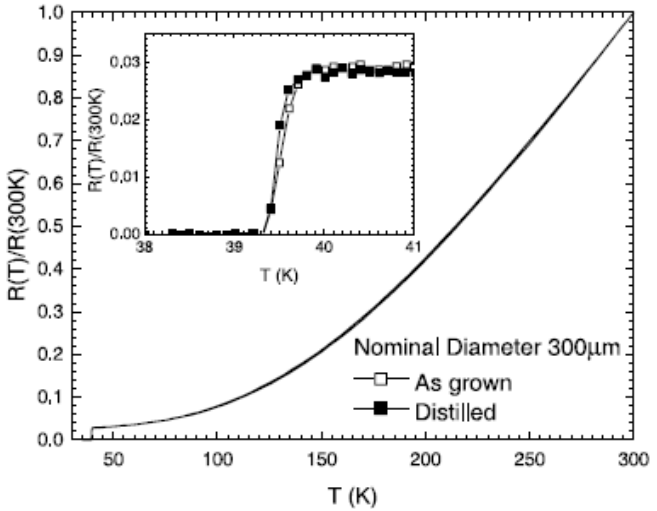

Physica B 382, 194 (2002)

Control of Defect Scattering

If the defect density of a compound can be controlled then ρ_0 (and therefore mean free path) can be systematically changed, leading to a constant off-set in resistivity curves. This can be done by annealing of the sample (in some cases).

Superconductivity is easy to spot in r(T) data since it manifests as a sudden drop in r to zero.

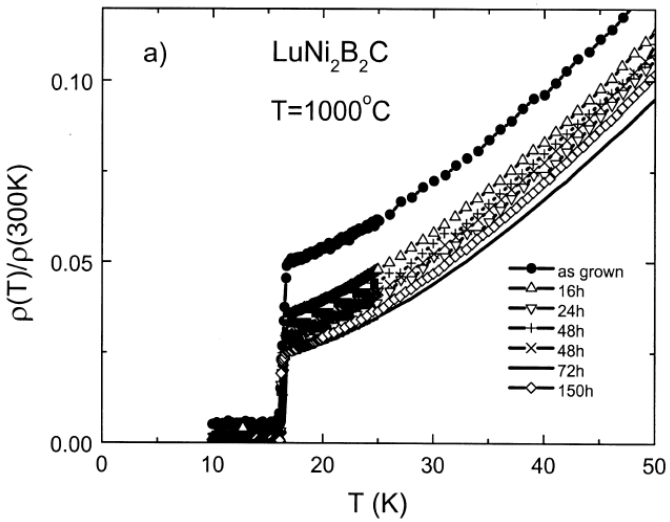

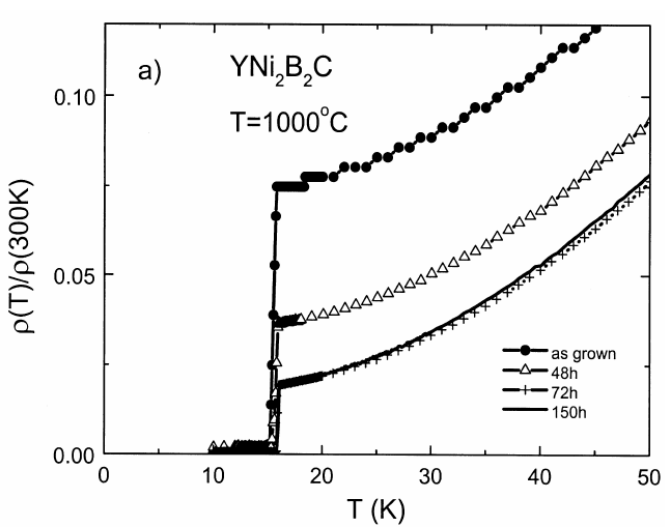

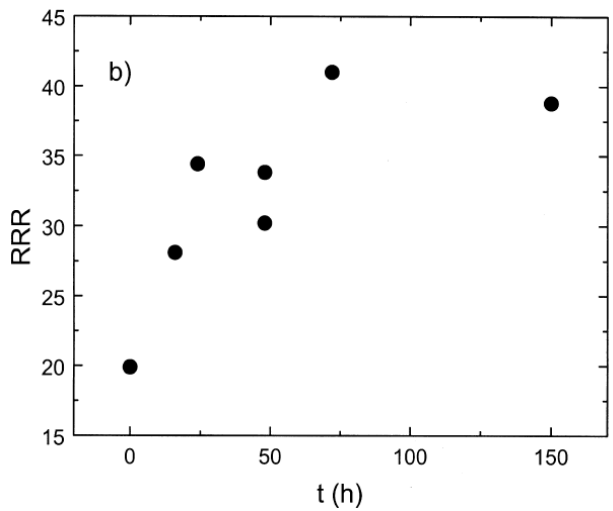

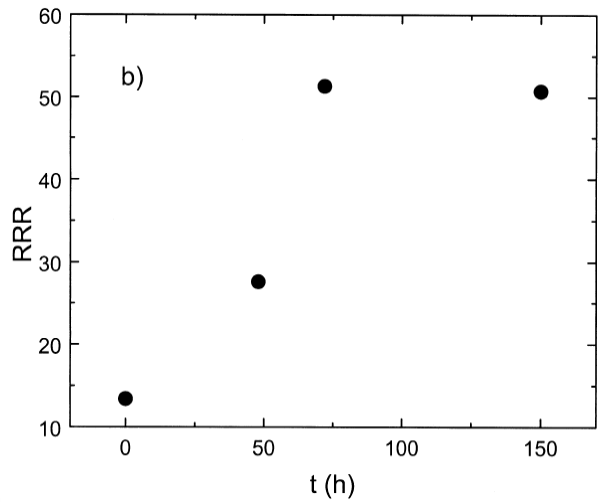

X.Y. Miao et al. / Journal of Alloys and Compounds 338 (2002) 13–19

(Courtesy of Paul Canfield, (Ameslab Iowa State))

Hall Effect Measurement

Charge carriers with charge e experience a Lorentz force that produces accumulation:

$$F_B = qvB$$

This produces a Hall field E_H that creates a force opposite to the Lorentz force:

$$F_E = qE_H$$

When two forces are equal, equilibrium is reached so we can determine the drift speed:

$$qvB = qE_H \Rightarrow v = \frac{E_H}{B}$$

Therefore current density is: $J = nqv = \frac{nqE_H}{B}$

We define Hall coefficient as:

$$R_H = \frac{E_H}{JB} = \frac{1}{nq}$$

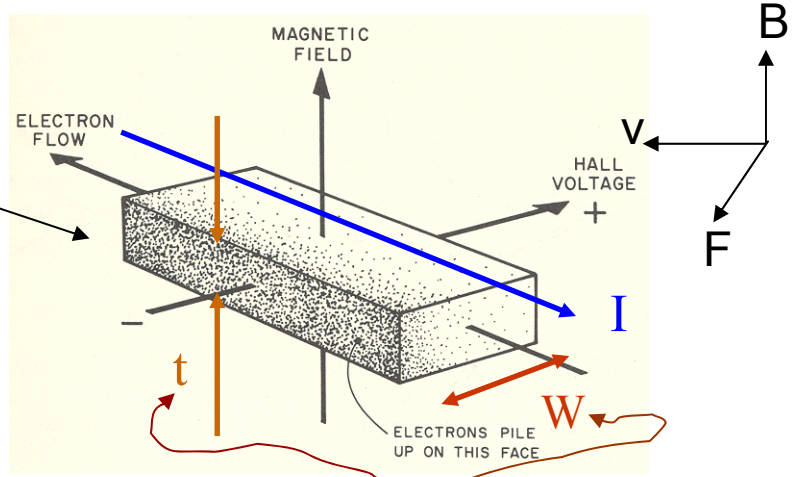

Experiment measures the Hall voltage $V_H = E_H w$ and the current $I = JA = Jwt$, so we can write:

$$R_H = \frac{E_H}{JB} = \frac{V_H / w}{(I / wt)B} = \frac{V_H t}{IB} = \frac{1}{nq}$$

Since $q = \pm e$ one can estimate carrier concentration n. Sign of V_H (R_H) can tell electron vs. holes

Hall angle: $$\tan\theta_H = \frac{E_y}{E_x} = \frac{J_x B_z}{E_x nq} = \frac{\sigma_x B_z}{nq} = \frac{q\mu_x B_z}{|q|}$$

And Hall mobility of charge carriers: $\mu_H = \sigma |R_H|$:

Hall Effect in Two Carrier Systems

Carrier system: set of carriers with same mobility, associated with one energy or degenerate levels

Hall coefficient can be expressed as:

$$R_H = \frac{\rho_{xy}}{H} = \rho_0 \frac{\alpha_2 + \beta_2 H^2}{1 + \beta_3 H^2}$$

Where α and β are functions of individual band mobility μ_1,μ_2 and carrier concentrations n_1,n_2 (J. Appl. Phys. 3187 (1999)):

$$\alpha_2 = f_1\mu_1 + f_2\mu_2; \beta_2 = (f_1\mu_2 + f_2\mu_1)\mu_1\mu_2$$
$$\beta_3 = (f_1\mu_2 + f_2\mu_1)^2; f_i = |n_i\mu_i| / \sum |n_i\mu_i|$$

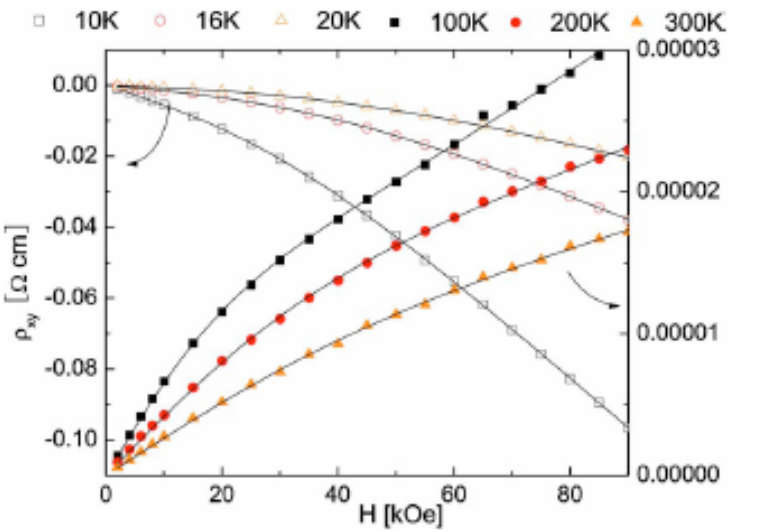

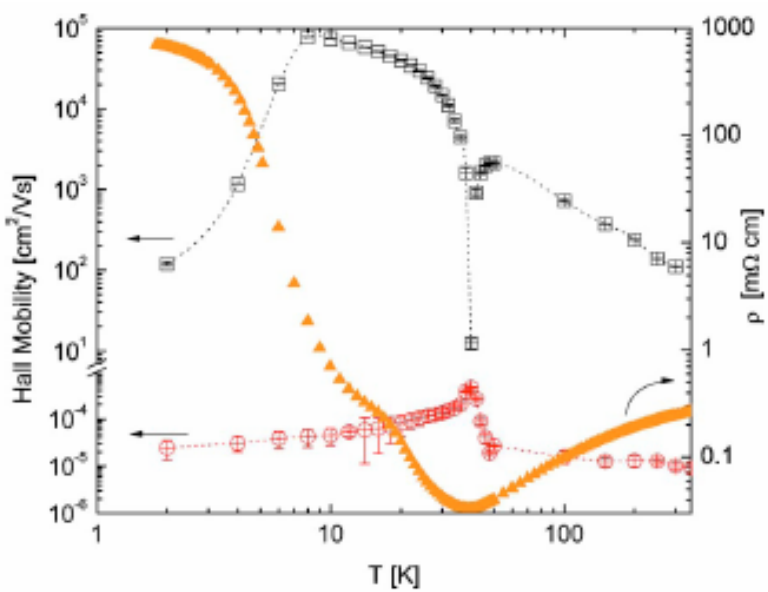

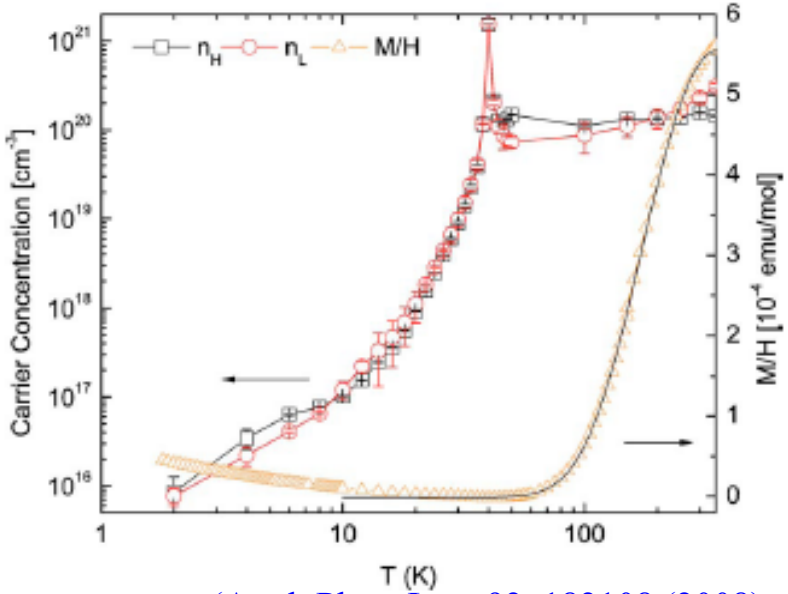

(Appl. Phys. Lett. 92, 182108 (2008)

Anomalous Hall Effect in Magnetic Materials

In ferromagnetic metals there is additional contribution to Hall resistivity due to M:

$Sb_{2-x}Cr_xTe_3$

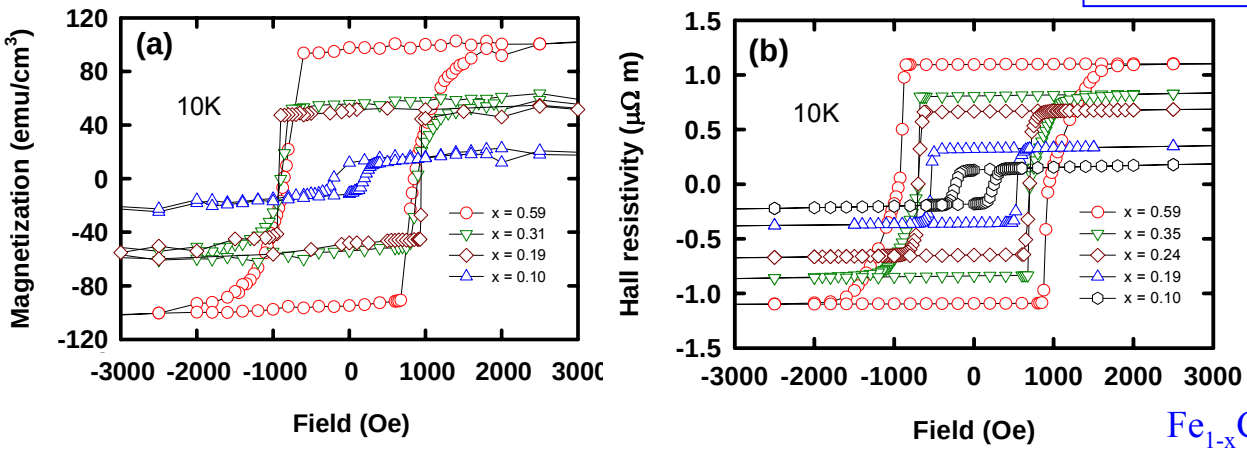

Normal Hall coefficient (dominant in high fields)

$$\rho_H = R_0 B + 4\pi R_s M$$

Anomalous Hall coefficient
$R_S \sim \rho^2$ (side jumps)
$R_S \sim \rho$ (skew scattering)
Berry phase

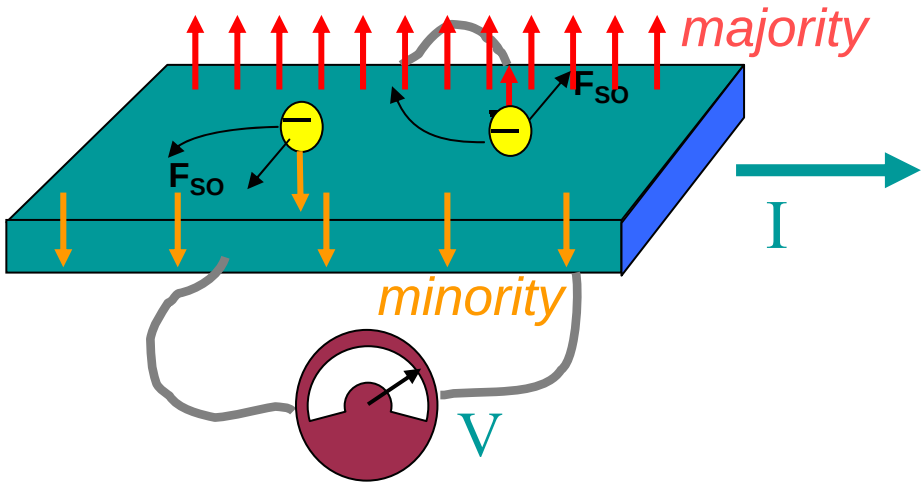

Coupling of orbital motion with spin magnetization (spin orbit coupling)

$Fe_{1-x}Co_xSi$: Phys. Rev. B 72, 224431 (2005)

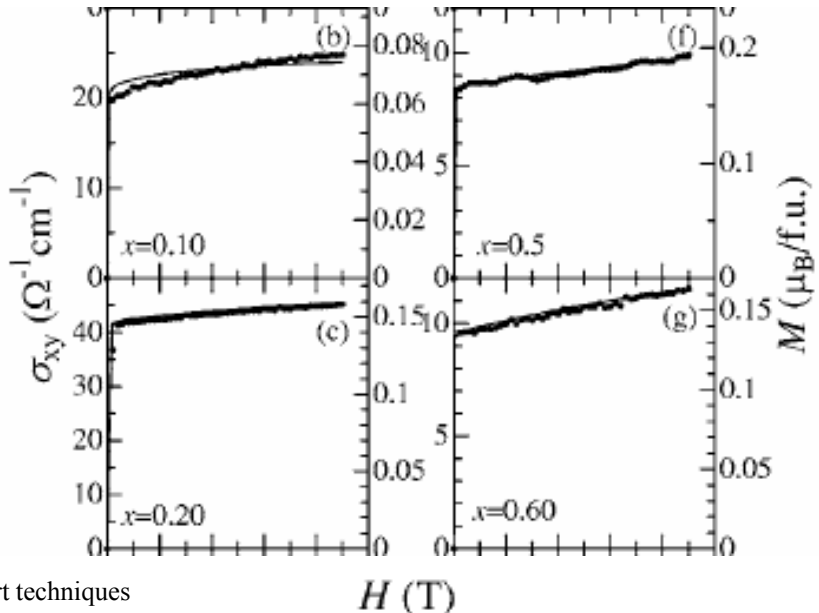

AC Transport option PPMS

Current source and a voltmeter in tandem, with AC bias current 1Hz to 1kHz. Pickup voltage is filtered and only same frequency and form signals are picked up, therefore reducing sources of noise. Four types of measurement: resistivity, Hall effect, I-V curves and critical current.

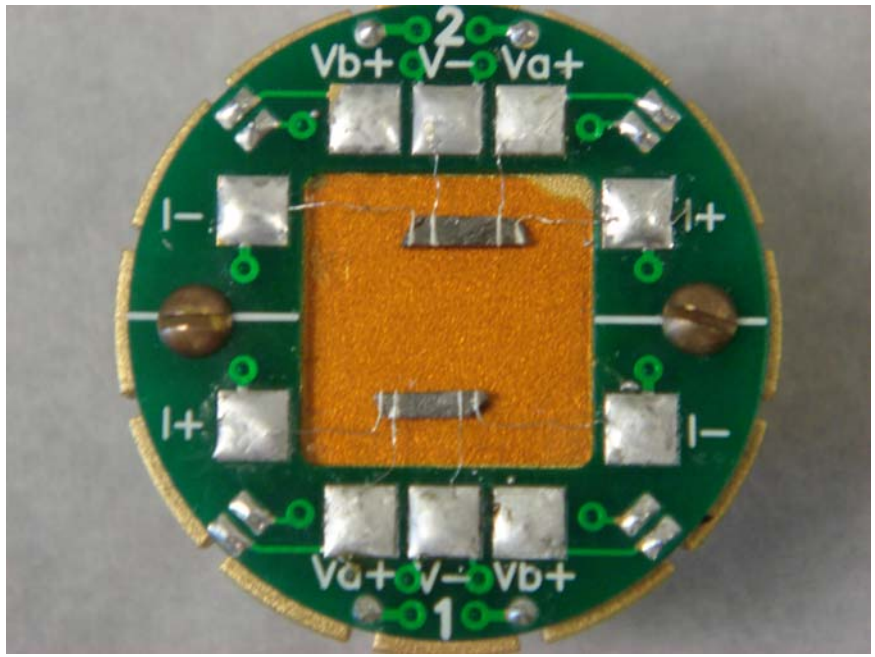

Samples mounted on ACT puck (Petrovic lab BNL)

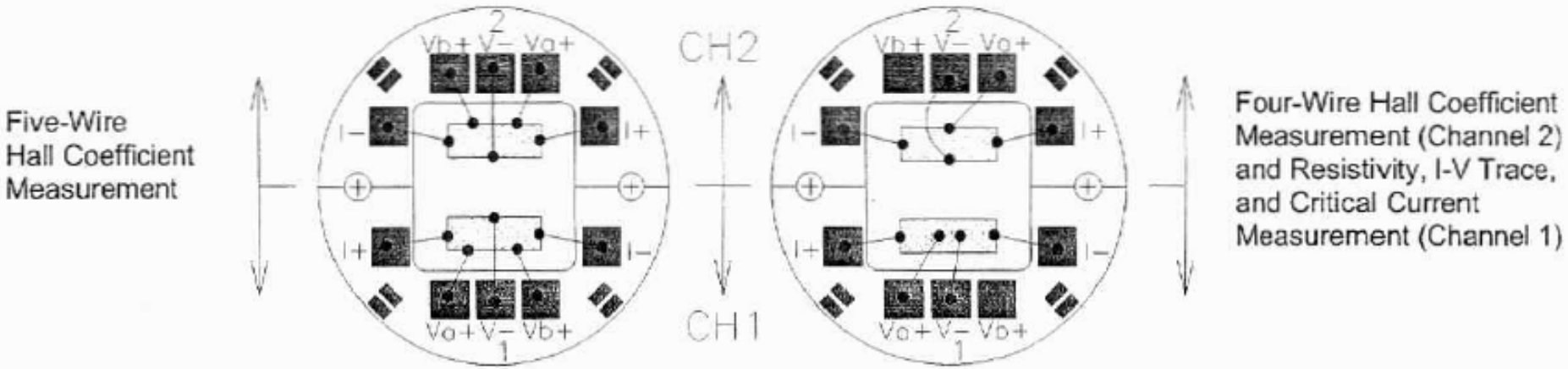

Hall Resistivity Sample Mounting in PPMS

Hall voltage is superimposed on bias voltage (>> V_H) from two leads which are not perfectly perpendicular, therefore we use 5 wire configuration.

With magnetic field turned off, potentiometer between two leads is used to adjust and null the offset due to sample resistance.

Offset voltage is further reduced by performing negative field sweeps and eliminating parasitic voltage just like thermal emf's.

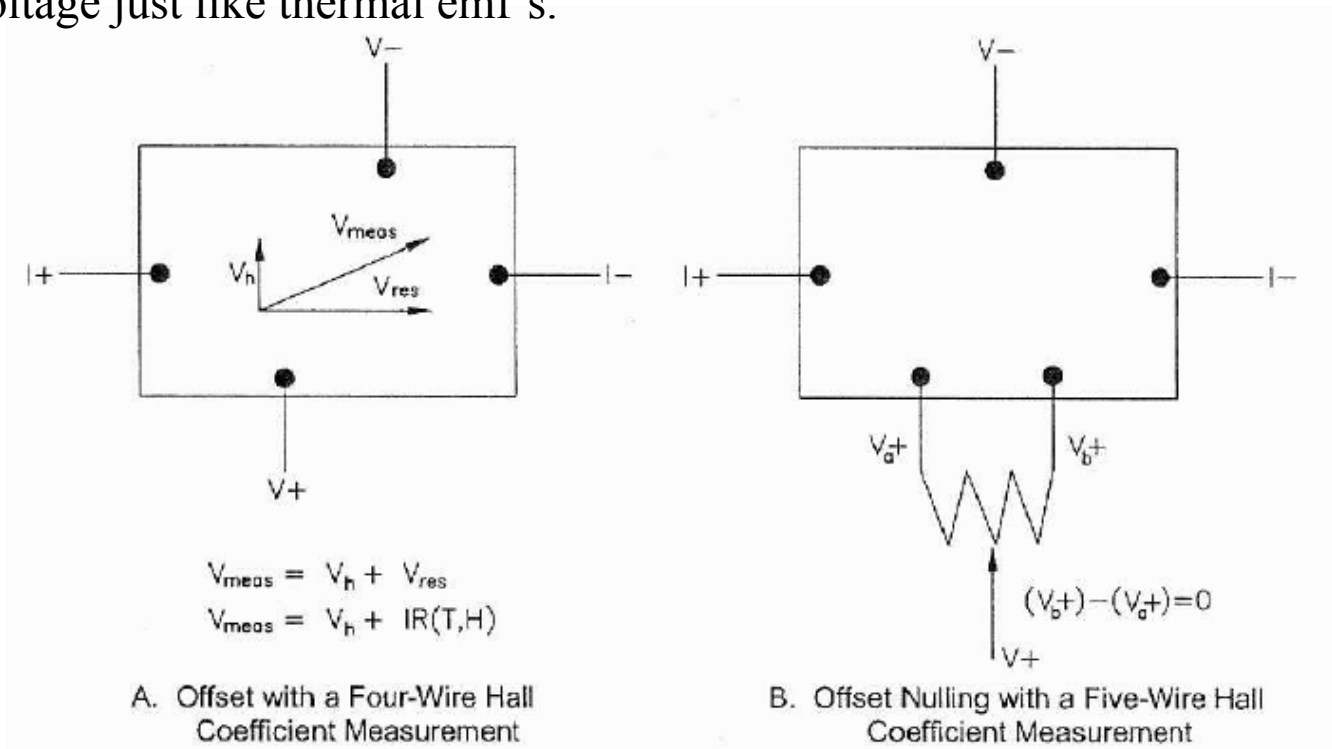

Effects of Local Moments

Residual resistivity ρ_0 decreases with increased order. Structurally this means less defects. The conduction electrons can also couple to localized magnetic moments, such as on rare earths.

When the moments change from disorder (paramag.) to order (ferromag., antiferromag., or more complex order) there is a scattering decrease - a loss of spin-disorder scattering. **Size of ordered moment matters, degree of hybridization, other scattering sources, etc..!**

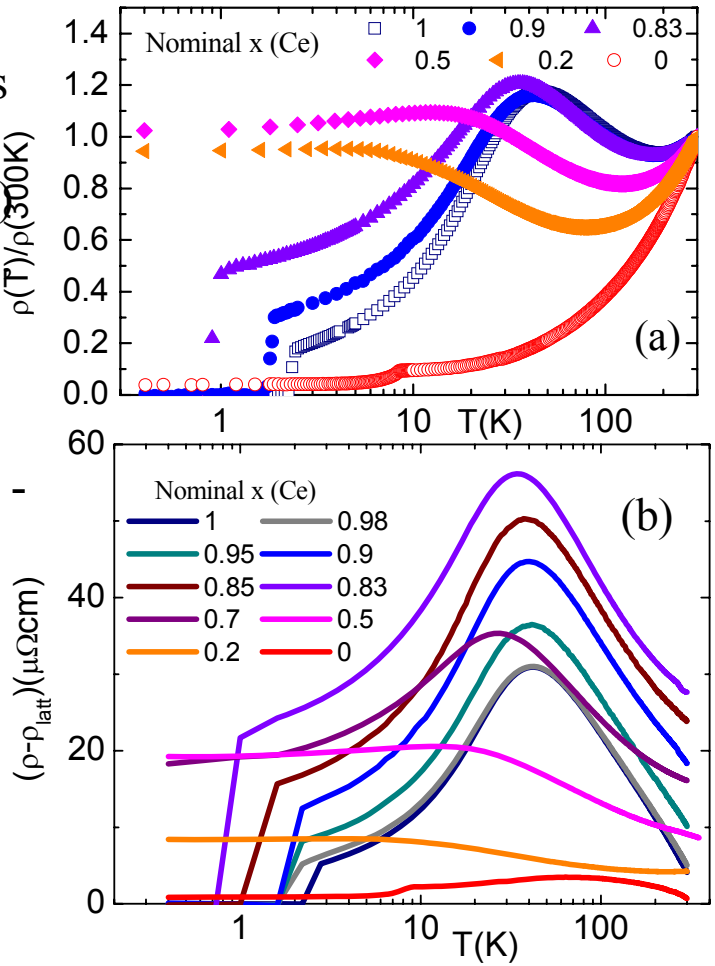

Phys. Rev. B 77 165129 (2007)

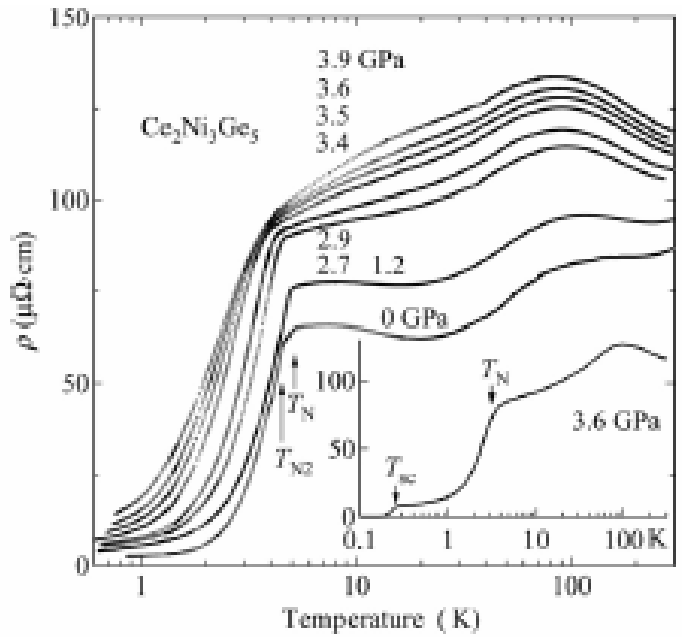

J. Phys. Cond. Matter 17, 4539 (2005)

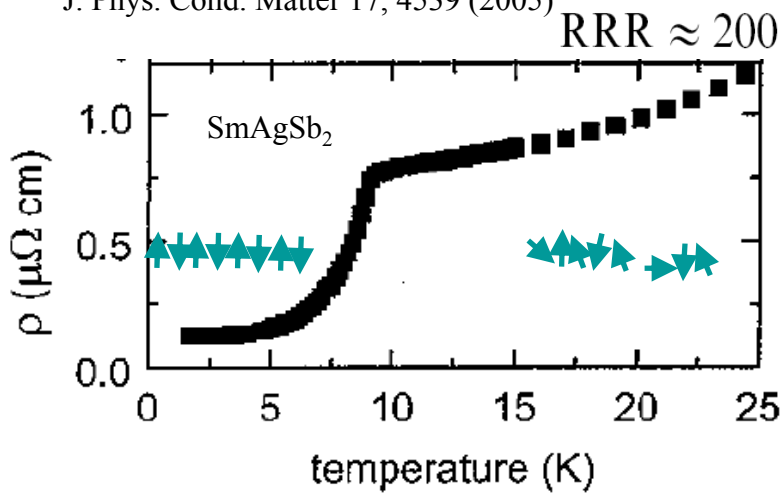

J. Magn. Magn. Mater 205, 27 (1999)

Resistivity of Multiple Transitions

Multiple transitions can be easily detected and identified: In this case we have a rare example of $T_N \sim 10$ K with the loss of spin disorder scattering, followed at lower temperatures by $T_c \sim$ 6K and a total loss of resistivity.

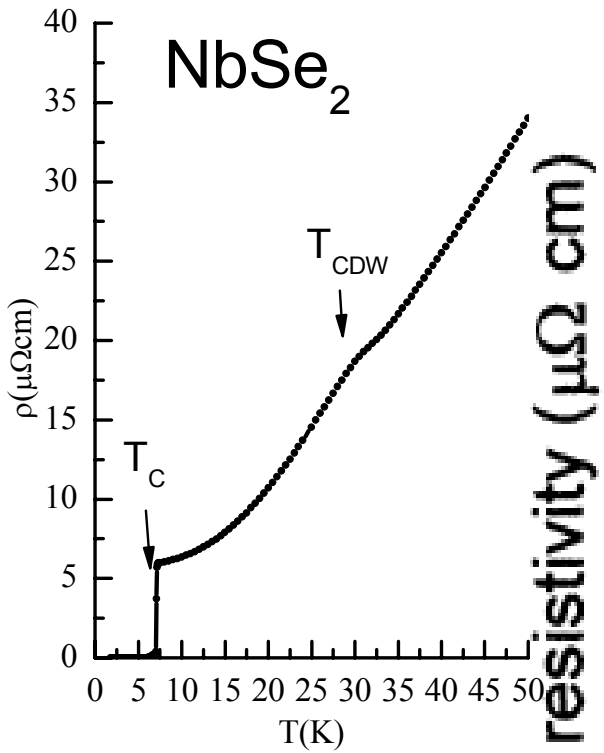

Resistivity detects Fermi surface changes.

CDW (and SDW) transitions: nested parts of the Fermi surface become gapped below T_{CDW}. For a partial gapping the sample remains metallic

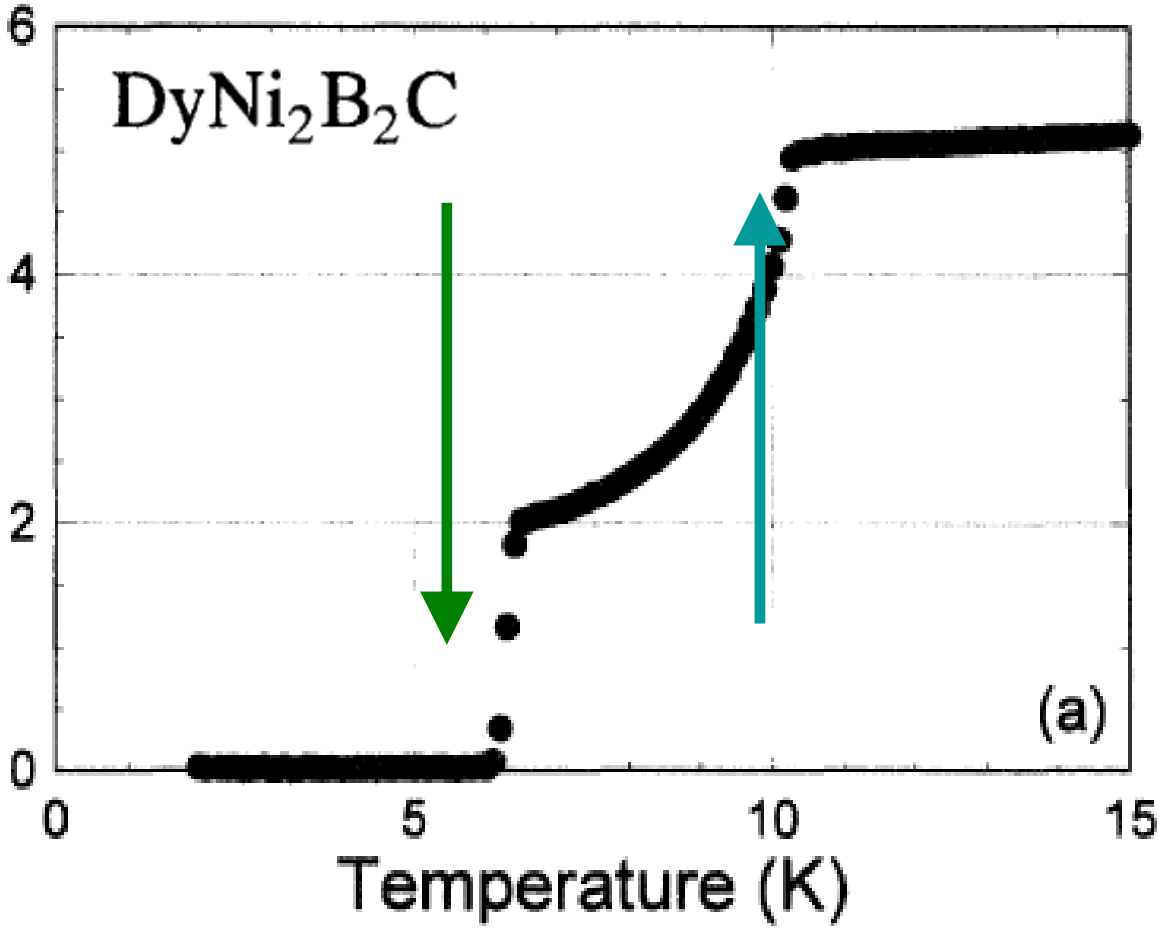

Phys. Rev. B 52, R3844 (1995)

Thermal Conductivity of Electrons

Heat flux due to change of entropy dS: dQ=TdS=dU-μdN → total flux: $\vec{J}_Q = \vec{J}_U - \mu\vec{J}_N$

Note single band is involved, sumation is necessary if more

$$J_U = \frac{1}{4\pi^3}\int \varepsilon(\vec{k})v(\vec{k})f(\vec{k})d\vec{k}; J_N = \frac{1}{4\pi^3}\int 1 \bullet v(\vec{k})f(\vec{k})d\vec{k} \Rightarrow J_Q = \frac{1}{4\pi^3}\int \left(\varepsilon(\vec{k})-\mu\right)v(\vec{k})f(\vec{k})d\vec{k}$$

We again apply relaxation time approximation, just like for σ, but here E=0 and spatial variation of f is due to T gradient $\nabla_r f_0 = \nabla_r T \bullet \partial f_0 / \partial T$ so we have :

$$f(\vec{k}) \approx f_0(\vec{k}) - \tau(\vec{k})\vec{v}\nabla_r f_0(\vec{k})$$

$$J_{Q,x} \approx \frac{1}{4\pi^3}\int \left(\varepsilon(\vec{k})-\mu\right)v_x^2(\vec{k})\tau(\vec{k})\frac{\partial f_0}{\partial T}\left(-\frac{\partial T}{\partial x}\right)d\vec{k}$$

$$\rho(\varepsilon) = \frac{1}{4\pi^3}\int_{\varepsilon(\vec{k})=const}\frac{dS_\varepsilon}{\nabla_k\varepsilon}; \left\langle v_x^2\right\rangle = v^2/3;$$

Let's evaluate this part:

$$\frac{1}{4\pi^3}\int v_x^2(\vec{k})\tau(\vec{k})\frac{\partial f_0}{\partial T}\left(-\frac{\partial T}{\partial x}\right)d\vec{k} = \frac{1}{4\pi^3}\int v_x^2(\vec{k})\tau(\vec{k})\frac{\partial f_0}{\partial T}\left(-\frac{\partial T}{\partial x}\right)\frac{dS_\varepsilon}{\nabla_k\varepsilon}d\varepsilon$$

Expressing this over density of states per volume

Now τ(ε)=τ(ε_F), v=(ε)=v(ε_F), const. and $\int \varepsilon\rho(\varepsilon)\frac{df_0}{dT}d\varepsilon = \frac{\partial}{\partial T}\int \varepsilon\rho(\varepsilon)f_0(\varepsilon)d\varepsilon = C_v$

We get: $\vec{J}_Q = -\kappa\nabla_r T \Rightarrow \kappa = \frac{1}{3}v_F^2\tau(\varepsilon_F)C_v$

T dependence governed by C_V and τ.

Thermal Conductivity in Metals

At low T electronic contribution or defect scattering is dominant → $\kappa \sim T$
At high T phonons are dominant
For $T < \theta_D$ $\tau_{ph} \sim T^{-3} \rightarrow \kappa \sim T^{-2}$
For $T > \theta_D$ $\tau_{ph} \sim T^{-1} \rightarrow \kappa \sim T$ ind.

We know $C_V \sim T$ for electrons

$$k_e = \frac{1}{3} C_e v_F \ell_e = \frac{1}{3} C_e v_F^2 \tau_e$$

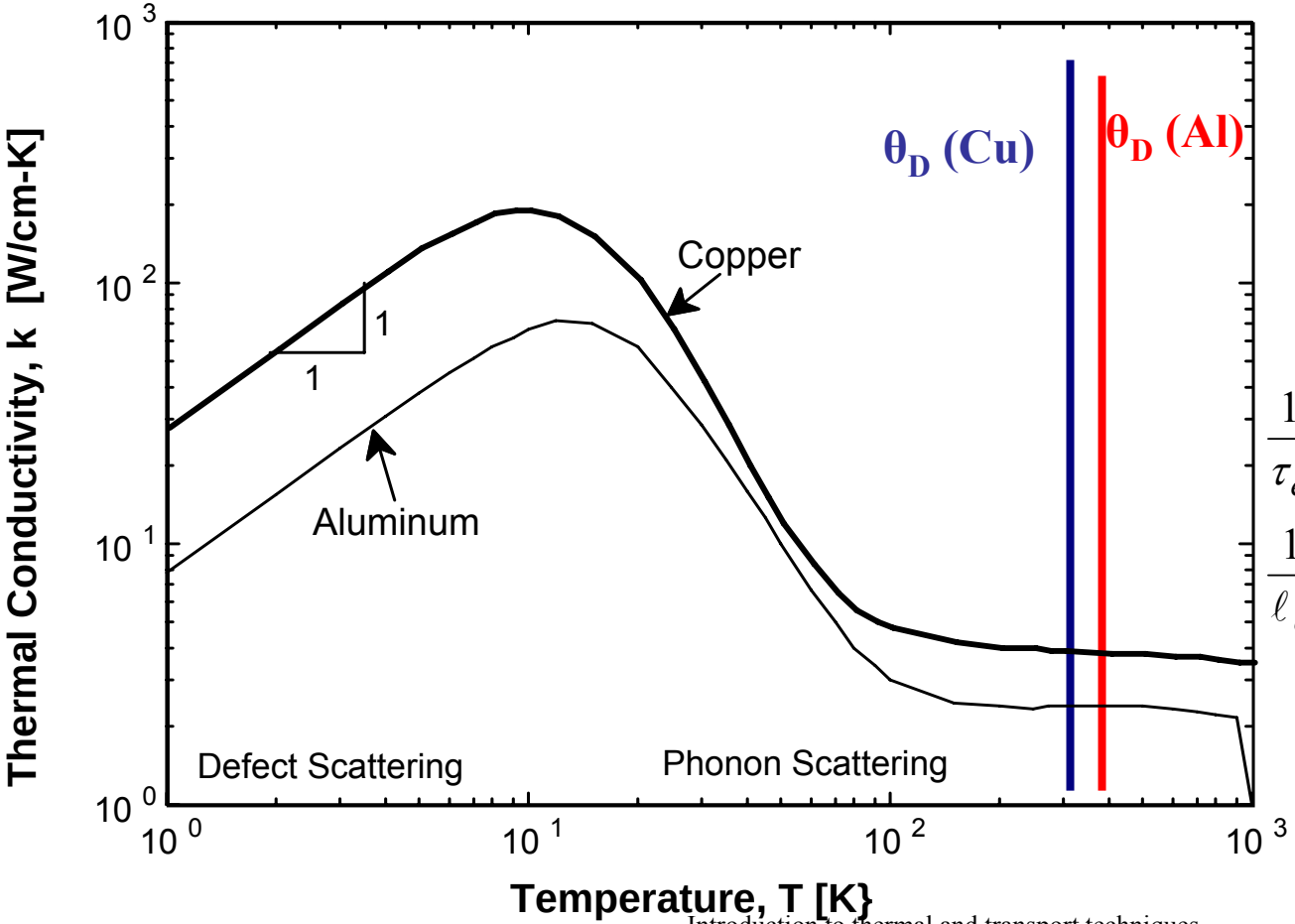

Matthiessen Rule:

$$\frac{1}{\tau_e} = \frac{1}{\tau_{defect}} + \frac{1}{\tau_{boundary}} + \frac{1}{\tau_{phonon}}$$

$$\frac{1}{\ell_e} = \frac{1}{\ell_{defect}} + \frac{1}{\ell_{boundary}} + \frac{1}{\ell_{phonon}}$$

Thermal Conductivity of Phonons

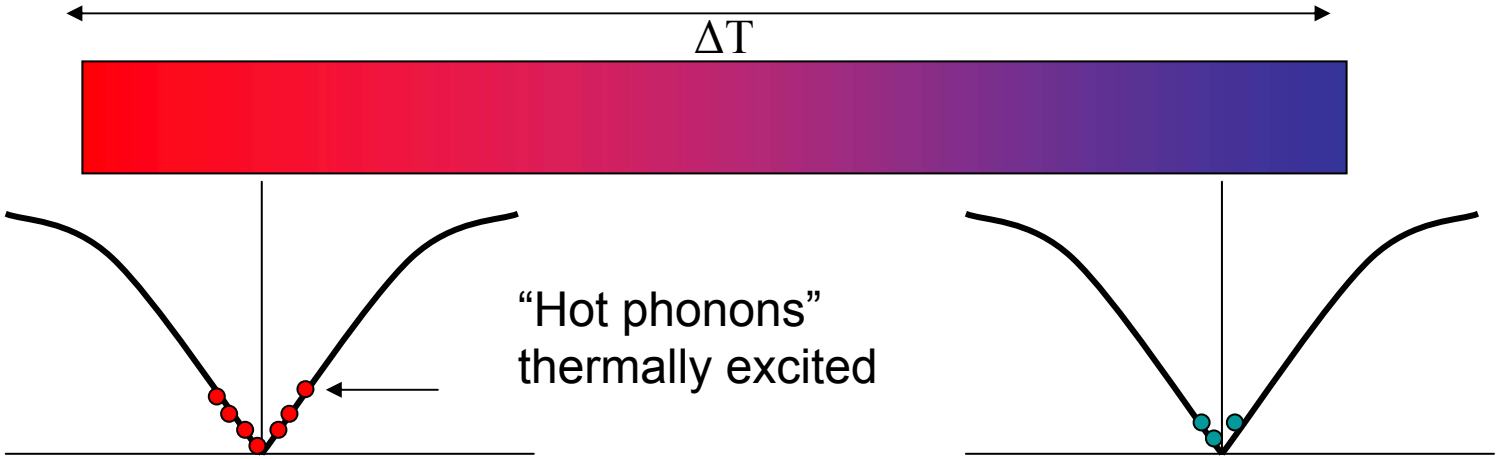

$$\vec{J}_Q = -\kappa \nabla T$$

On the "Hot" side phonons with higher energy are excited while on the other side only low energy phonons are excited by establishment of thermal gradient.

The high-energy phonons propagate from left to right at the phonon velocity. Phonon thermal conductivity can be decreased by phonon scattering – dislocations in the crystal lattice, grain boundaries, impurities, etc..

Thermal conductivity in metals has electron and phonon part, in insulators there are no electrons thus thermal conductivity comes from the phonons.

T variation produces non-equilibrium distribution of phonons that propagate with group velocity v_g in a wave packet with $|\Delta k| \sim 1/\Delta x$

Thermal Conductivity of Phonons

Harmonic approximation: wave packet will travel without scattering since phonons are independent normal modes → κ is infinite. However, structural defects, surfaces, grain boundaries..are causes of scattering that changes phonon momentum. We look for **heat flux J_Q – sum of energies carried by all phonon modes ·v_g:**

$$J_Q = \frac{1}{V}\sum_{k,p} n(\vec{k},p)\hbar\omega_k \vec{v}_g(\vec{k},p) = \frac{1}{V}\sum_{k,p} \hbar\omega_k(p)\left(n-n^0\right)_{k,p}\vec{v}_g(\vec{k},p)$$

Phonon occupation #

In equilibrium no T gradient, J=0 since $v_g(\mathbf{k})=v_g(-\mathbf{k})$ for all crystal directions and $n(\mathbf{k},\mathbf{p})=n_0(\mathbf{k},\mathbf{p})$ so difference from equilibrium is needed

Change in phonon number is: $\frac{dn_{k,p}}{dt} = \left.\frac{\partial n_{k,p}}{\partial t}\right|_{diffusion} + \left.\frac{\partial n_{k,p}}{\partial t}\right|_{decay}$

diffusion in and out of some region and decay in other phonons

Phonon (not heat) flux $J_{k,p}=n_{k,p}v_g(k,p)$

Steady state (quasi equilibrium)

$$\left.\frac{\partial n_{k,p}}{\partial t}\right|_{diffusion} = -\nabla J_{k,p} = -\vec{v}_g(\vec{k},p)\nabla n_{k,p} = -\left(\frac{\partial n^0_{k,p}}{\partial T}\right)\vec{v}_g(\vec{k},p)\nabla T$$

$$\left.\frac{\partial n_{k,p}}{\partial t}\right|_{decay} = -\frac{\left(n_{k,p}-n^0_{k,p}\right)}{\tau_{k,p}}$$

0

And we have: $\left[n-n^0\right]_{k,p} = \tau_{k,p}\frac{dn_{k,p}}{dt} = -\tau_{k,p}\left(\frac{\partial n^0_{k,p}}{\partial T}\right)\vec{v}_g(\vec{k},p)\nabla T$

Therefore for one crystal axis projection (again $\langle v_x^2\rangle = v^2/3$):

$$\kappa = \frac{1}{3V}\sum_{k,p}\hbar\omega_k(p)v_g^2(\vec{k},p)\tau(\vec{k},p)\frac{\partial n^0_{k,p}}{\partial T} = \frac{1}{3V}\sum_{k,p}C_V(\vec{k},p)\Lambda_{k,p}v_g(\vec{k},p)$$

Mean free path of phonon mode

$$\Lambda_{k,p} = v_g(\vec{k},p)\tau_{k,p}$$

Thermal Conductivity of Phonons

Thermal Conductivities and Phonon Mean Free Paths

	($T = 273°K$) K, watt/m·°K	l, Å	($T = 20°K$) K, watt/m·°K	l, cm
SiO_2 (quartz)	14	97	760	7.5×10^{-3}
CaF_2	11	72	85	1.0×10^{-3}
NaCl	6.4	67	45	2.3×10^{-4}
Si	150	430	4200	4.1×10^{-2}
Ge	70	330	1300	4.5×10^{-3}

High temperatures: Phonon-phonon scattering controls Λ Phonons can interact with other phonons. Anharmonic coupling "mixes" the normal modes and leads to coupling of the phonons. At very low temperatures, only very long phonons (near k = 0) are excited. They do not couple well to defects or other imperfections (size mismatch) so Λ goes up as temp goes down, and at low temps becomes comparable to size of object

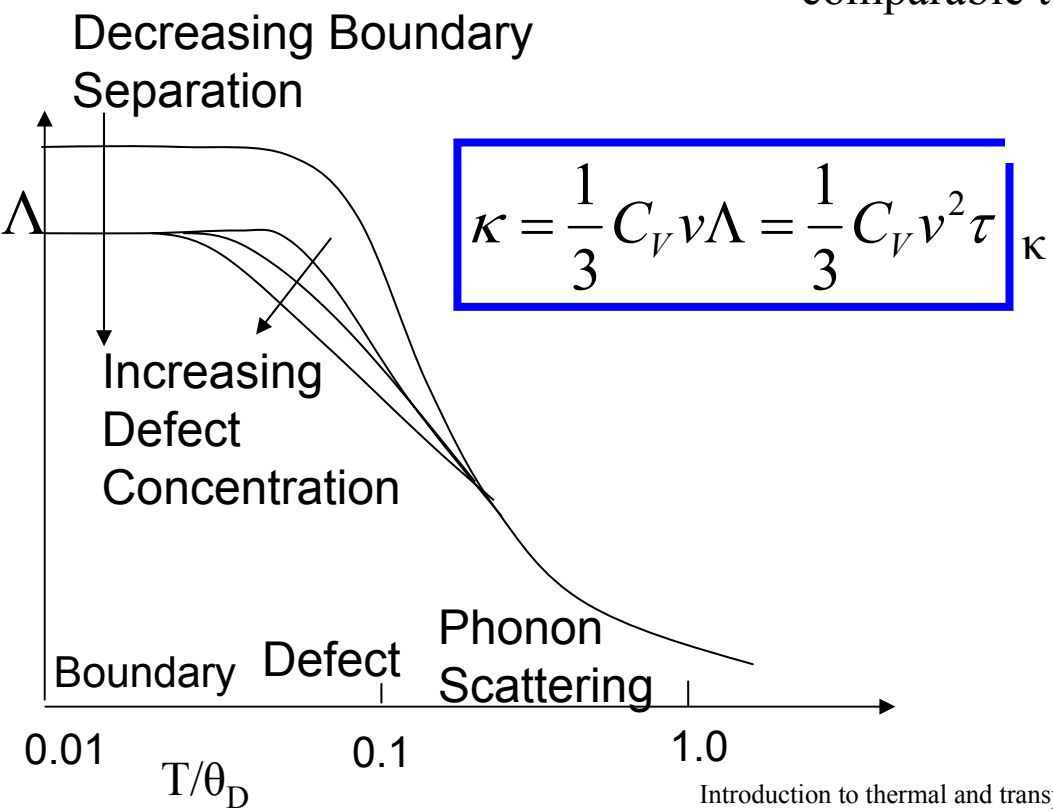

$$\kappa = \frac{1}{3} C_V v \Lambda = \frac{1}{3} C_V v^2 \tau$$

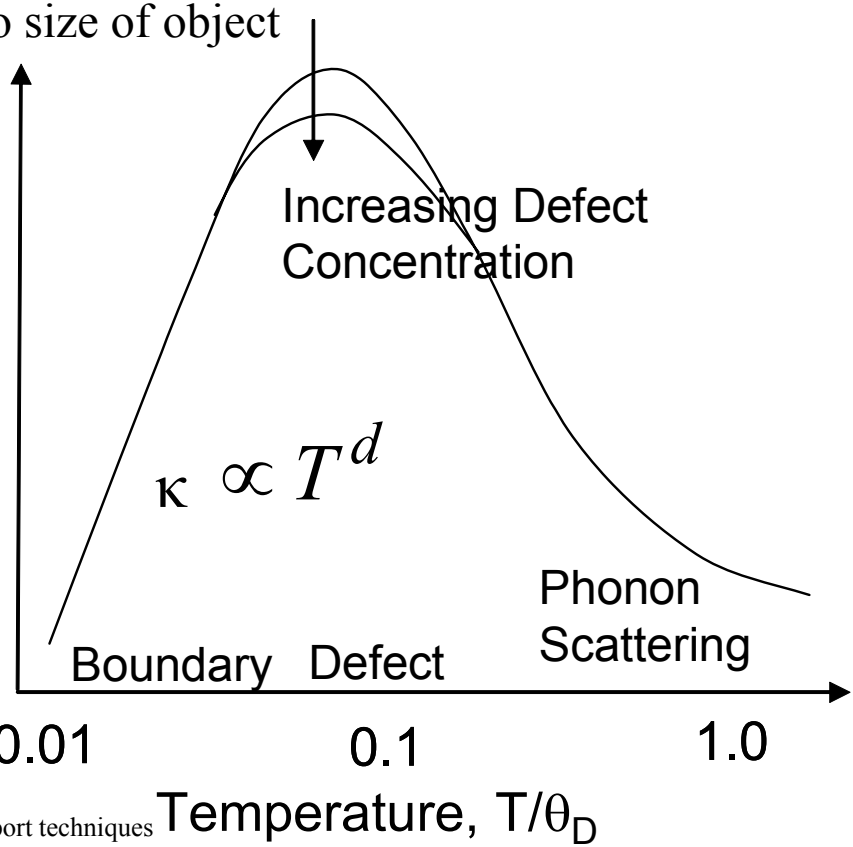

Thermal Conductivity Example

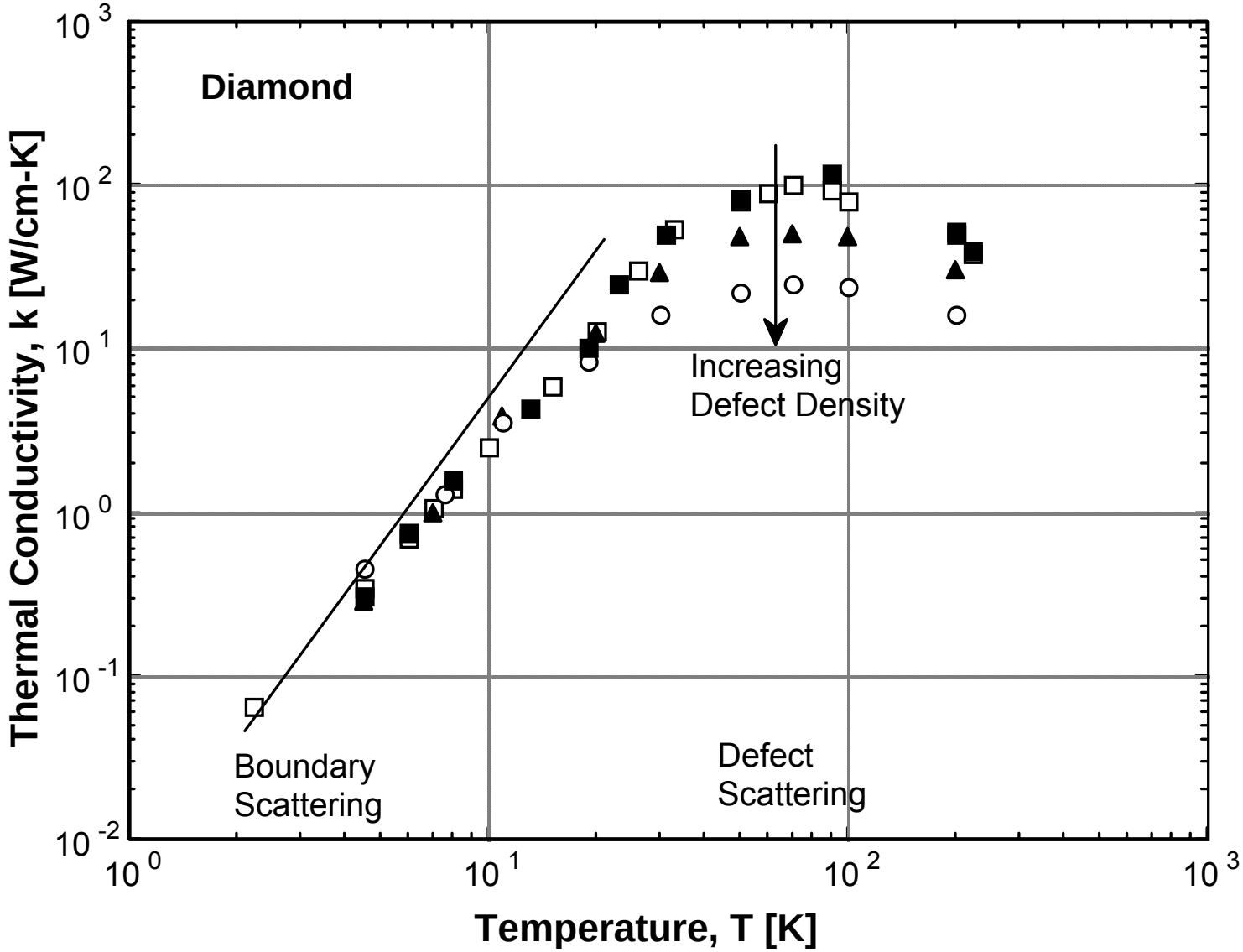

Mean Free Path and Electron Scattering

Wiedemann Franz law:

$$\frac{\kappa}{\sigma T} = L = \frac{\pi^2 k_B^2}{3e^2} = 2.45 \bullet 10^{-8} \frac{W\Omega}{K^2}$$

Valid in relaxation-time approximation, if some scattering mechanism reduces κ and σ with the same rate, for example Elastic scattering or inelastic where $\Delta\varepsilon << k_B T$. For example at T=0 (where electronic + defect mechanism dominates Or at $T >> \theta_D$ where phonons dominate. In intermedate range inelastic e^- - ph scattering Causes greater degradation of thermal currents since both electron ε and momentum are changed. **Note that at T=0 it does not depend on electronic interactions**

Electronic conductivity: $\sigma = ne^2\tau/m$

Thermal Conductivity $k_e = \frac{1}{3} C_e v_F \ell_e = \frac{1}{3} C_e v_F^2 \tau_e$

Scattering time $\tau_e = l_e / v_F$

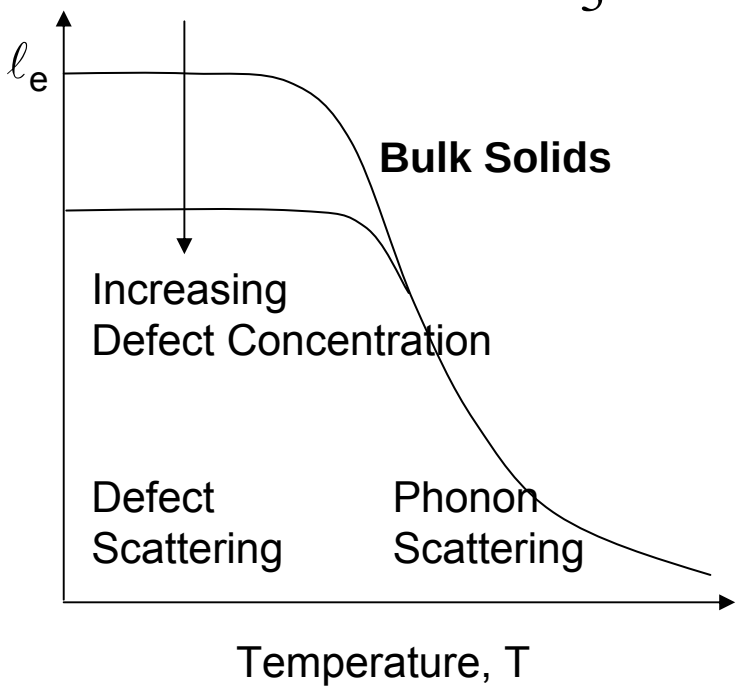

In polycrystalline materials

- Defect Scattering
- Phonon Scattering
- Boundary Scattering (Film Thickness, Grain Boundary)

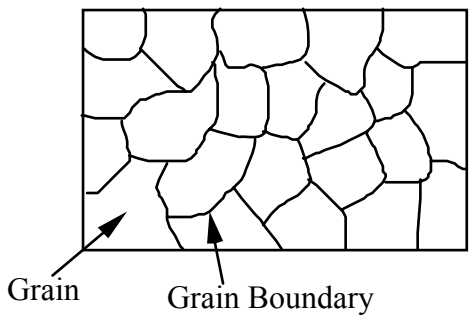

Thermal Transport Measurements: Steady vs. Pulse

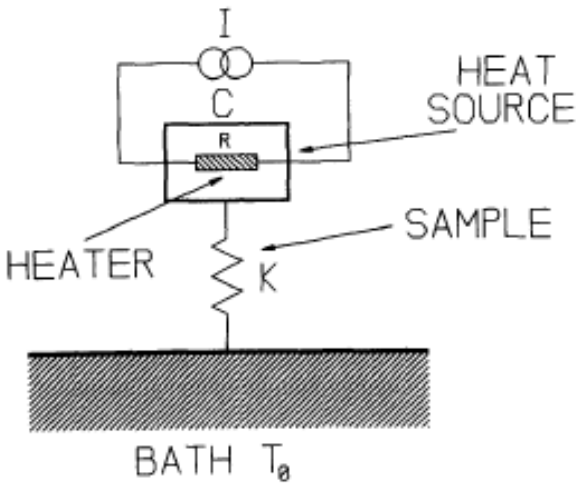

Figure 2 Schematic representation of experimental set-up: K = thermal conductance, C = thermal capacity, I = current source, T_0 = bath temperature

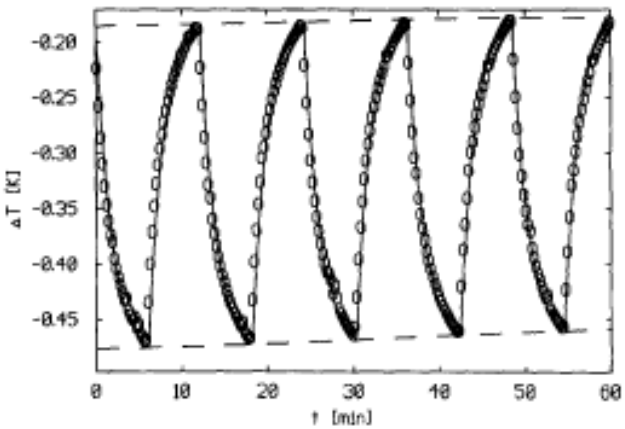

Figure 3 Time dependence of temeprature difference across the sample: (——) simulation; (O) experiment

Steady method: applying heat and measuring temperature (ΔT) and voltage gradients in equillibrium → wait times can be big due to T stabilization (that includes offset registration) and establishment of gradient

Pulse method: slow drift in bath T, heat current that generates temperature gradient is pulsed. Resulting signal is exponential for both ΔT and ΔV. We assume $\Delta T=(T_1-T_0) << (T_1+T_0)/2 = \overline{T}$

$$\frac{dQ}{dt} = C(T_1)\boxed{\frac{dT_1}{dt}} = I^2(t)R(T_1) - K(T_1 - T_0)$$

If one runs step – function I through heater, after some t equilibrium is reached where $dT_1/dt = 0$ so:

$$K(\overline{T}) = \frac{I^2 R(T_1)}{T_1 - T_0}$$

But if T_0 drifts slowly and if we let periodic square wave Through the heater where I = 0 for t = [$|2\tau<\tau|$] and I = I_0 for t = [$|2\tau\geq\tau|$], T of the system will be oscillatory with exponential solutions for $\Delta T(t)$. See

O. Maldonado, Cryogenics 32, 908 (1992)

Thermal Transport Measurements in PPMS 1

PPMS TTO option enables simultaneous measurement of thermal conductivity κ, Seebeck coefficient S (thermopower) and (AC) resistivity ↔ enables measurement of $Z = S^2/\kappa\rho$

Continuous measurement: taken continuously and software adjusts parameters (heater power and period) to optimize measurement.

Single measurement: slower, system reaches equilibrium with heater "on" and "off" before taking data point. No curve fitting is required. Less dependence on thermal history

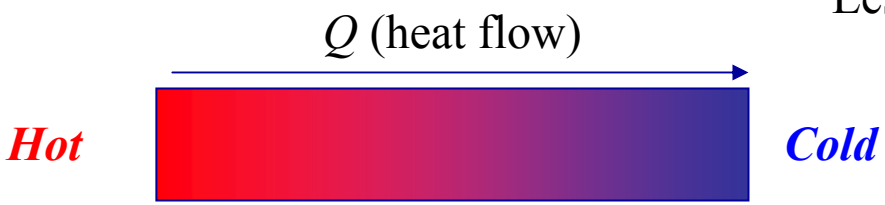

Measurement of κ: Heater applies heat, and ΔT is measured (W/mK):

$$\frac{\Delta Q}{\Delta t} = \kappa A \frac{\Delta T}{x} \Rightarrow \kappa = \frac{\Delta Q x}{\Delta t \Delta T A}$$

Measurement of S: Heater applies heat, and ΔV is measured (V/K):

$$S = -\frac{\Delta V}{\Delta T}$$

Measurement of ρ: Same as in ACT, same probes (leads) used for thermal and electrical measurements, electrical measurements are taken at the beginning and at the end of the heat pulse

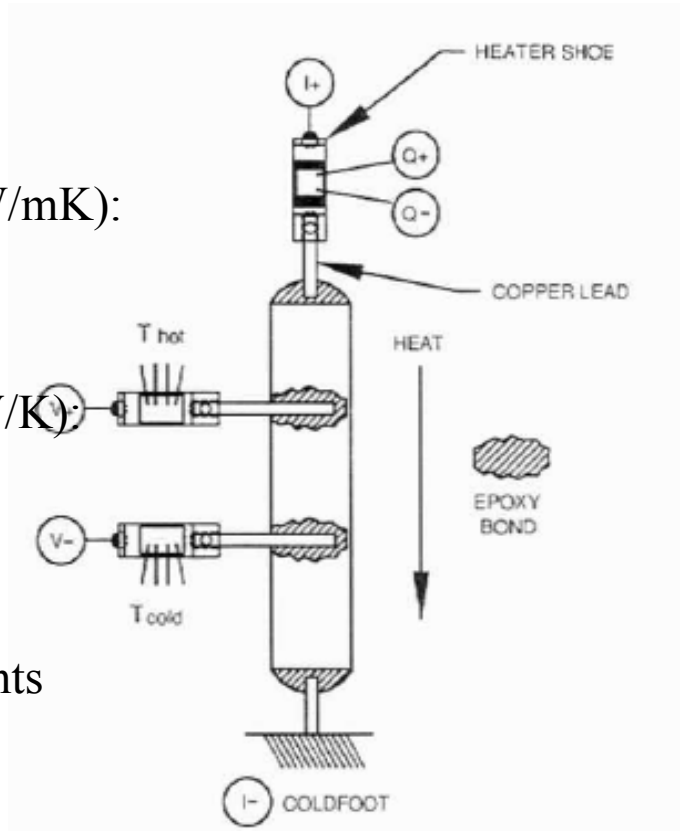

Thermal Transport Measurements in PPMS 2

Sample mounting: two probe and four probe measurement (3 - 10mm sample length).

High limit: heater power **P(W) = κΔT(A/l).** Since ΔT ~ 0.03T → **for P_{max} = 50mW some A/l of the sample limits measurable κ** → upper limit on A/l for fixed κ

Low limit: thermal diffusion time in the sample **τ = C_p/K** (K = conductance = κA/l)

In order not to have too long diffusion time there will be some **upper limit on τ** → some **low limit on A/l** for fixed κ: $\tau = C_p l^2/\kappa$

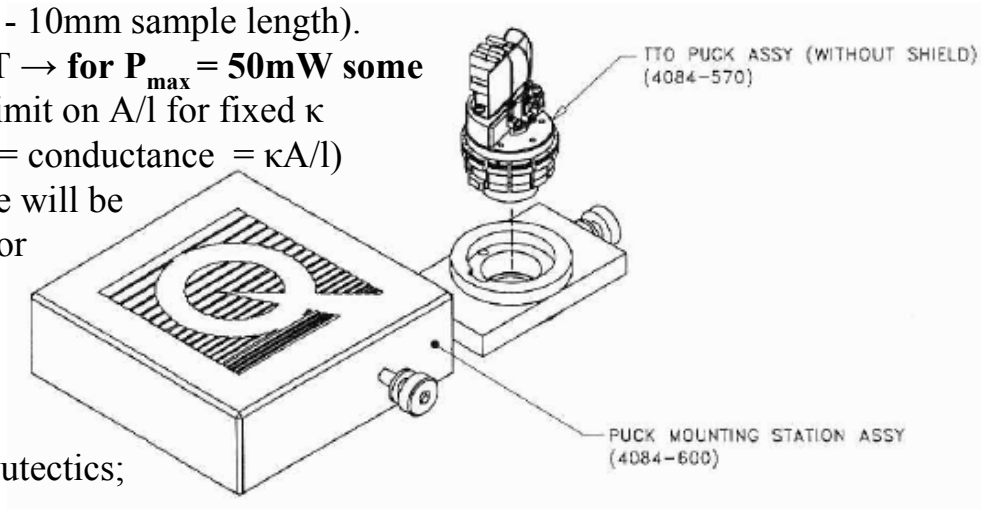

Gold plated Cu leads, grease to increase thermal contact.

Mounting Epoxies: Silver H20E, Tra-Bond816H01, metals, eutectics; thermal resistance increases at low T

Only if thermal and electrical resistance of sample is so high so that we can neglect contribution of leads.

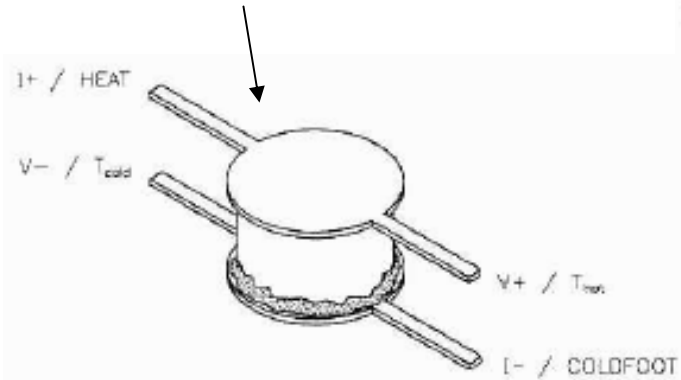

In all other cases one should use four probe method

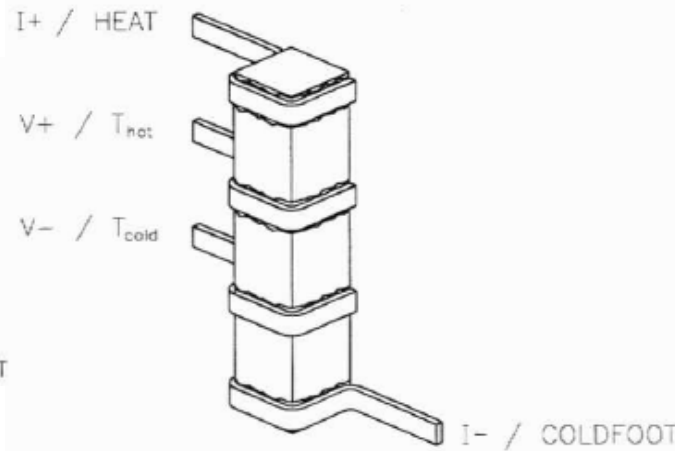

TTO 3

Continuous measurement: optimization of heater current, heat pulse period and R excitation.

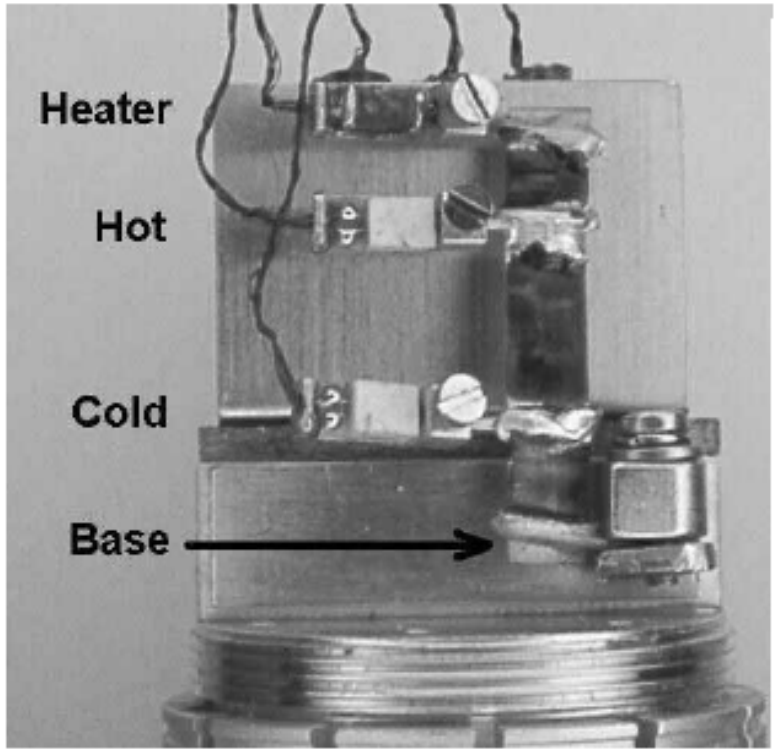

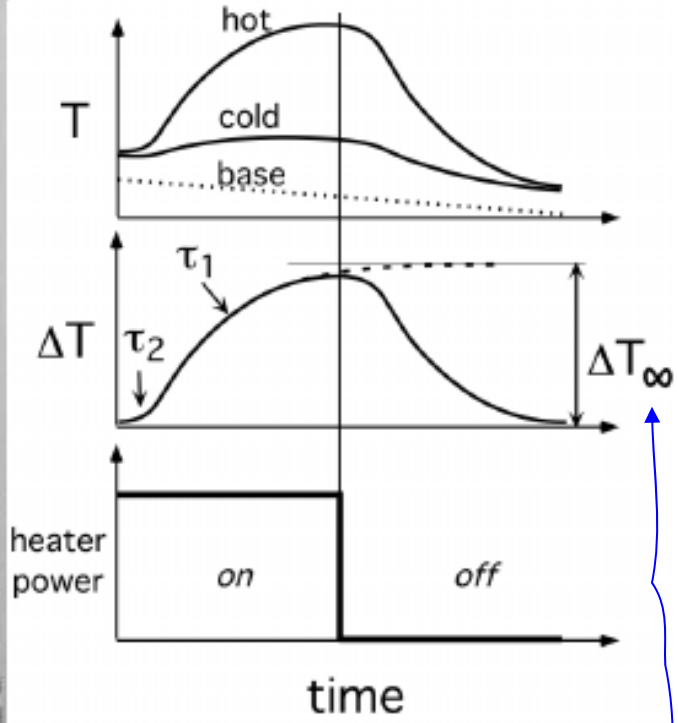

Least square fitting of these variables after ΔT vs time over the duration of the heat pulse data are obtained. Fitting routine searches for T_∞, τ_1 and τ_2:

$$\Delta T = \Delta T_\infty \left[1 - \frac{\tau_1 e^{-t/\tau_1} - \tau_2 e^{-t/\tau_2}}{\tau_1 - \tau_2} \right]$$

Asymptotic T drop across the sample

Cooling "pulse" is fitted with the profile:

constant

$$\Delta T_{cooling} = A - \Delta T_{cooling}$$

Thermal history is accounted in the model by taking into account two previous pulses.

Fitting for Seebeck voltage is similar:

$$\Delta V = \Delta V_\infty \left[1 - \frac{\tau_1 e^{-t/\tau_1} \pm \tau_2' e^{-t/\tau_2'}}{\tau_1 - \tau_2'} \right] + bt + c$$

Seebeck for leads (dominated by τ_2) may be different from sample S (dominated by τ_1)

Linear (account for varying thermal V) drift and offset voltage

Thermal Transport Measurement in PPMS 4

Errors in the measured quantities are calculated in the standard manner. For ΔT vs time curve it is calculated as:

$$R_{\Delta T} = \sqrt{\frac{\sum_i (\Delta T_i - \Delta T_{i,\mathrm{model}})^2}{N}}$$

Number of data points in the curve
N = 64 for κ, S and 128 for ρ

Error in sample radiation, 20% estimated combined error from emissivity and sample radiation

Heater current error

Standard deviation in thermal conductivity is:

$$\sigma(\kappa) = \kappa \sqrt{\left(\frac{R_{\Delta T}}{\Delta T_\infty}\right)^2 + \left(\frac{2IR\delta I}{P}\right)^2 + \left(\frac{0.2Ploss}{P}\right)^2 + \left(\frac{0.1T_\infty K_{shoes}}{P}\right)^2}$$

Thermal conductance leak from shoes assumed 10%

Voltage error:

$$\sigma(\alpha) = \alpha \sqrt{\left(\frac{R_{\Delta V}}{\Delta V_\infty}\right)^2 + \left(\frac{R_{\Delta T}}{\Delta T_\infty}\right)^2}$$

Resistivity error (average of beginning and end heat pulse measurement:

Peak to peak V

$$\sigma(\rho) = \rho \frac{R_\rho}{V_{pp}} = \frac{\rho}{V_{pp}} \sqrt{\frac{\sum_i (V_i - V_i, \mathrm{model})^2}{N}}$$

ZT error is simply: $\sigma(ZT) = ZT \sqrt{\left(\frac{2\sigma(S)}{S}\right)^2 + \left(\frac{\sigma(\kappa)}{\kappa}\right)^2 + \left(\frac{\sigma(\rho)}{\rho}\right)^2 + \left(\frac{\sigma(T)}{T}\right)^2}$

Heat loss errors: $K[W/K] = \frac{(I^2R - P_{rad})}{\Delta T - K_{shoes}}$

$P_{rad} = \sigma_T (A_{total}/2) \varepsilon (T_{hot}^4 - T_{cold}^4)$

$K_{shoes} = aT + bT^2 + cT^3)$

½ of surface area is radiating, the other is cold

σT – Stefan – Boltzmann constant
5.67·10-8 (W/K⁴m²

ε – infrared emissivity, important above 300 K since some Radiative heat power is lost To surrounding heat shield

TTO Calibration Files

Relative errors in measurement can be ~ 10 - 20%, above 300K (radiation heating) and when measuring small κ. Note that errors become large near large changes, phase transitions (metal – insulator in this case).

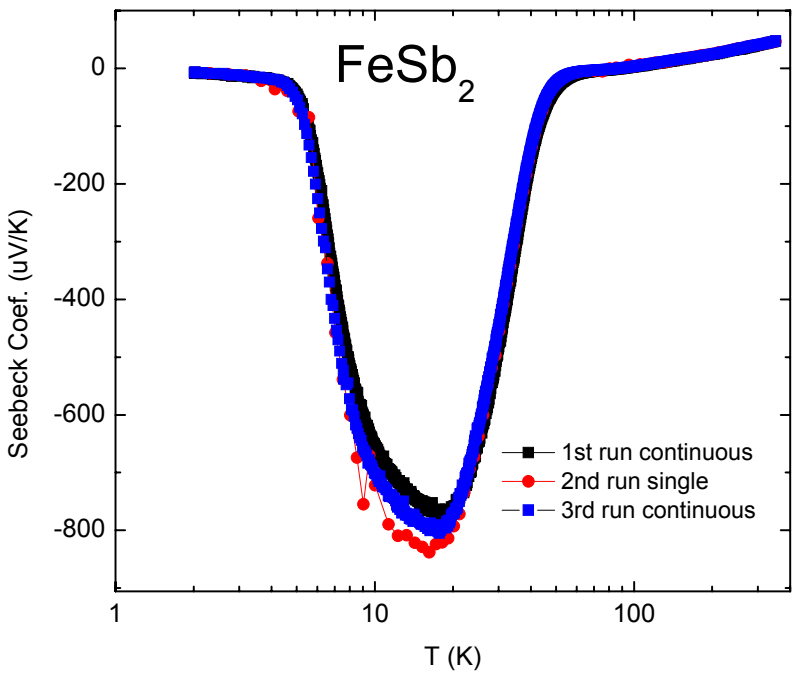

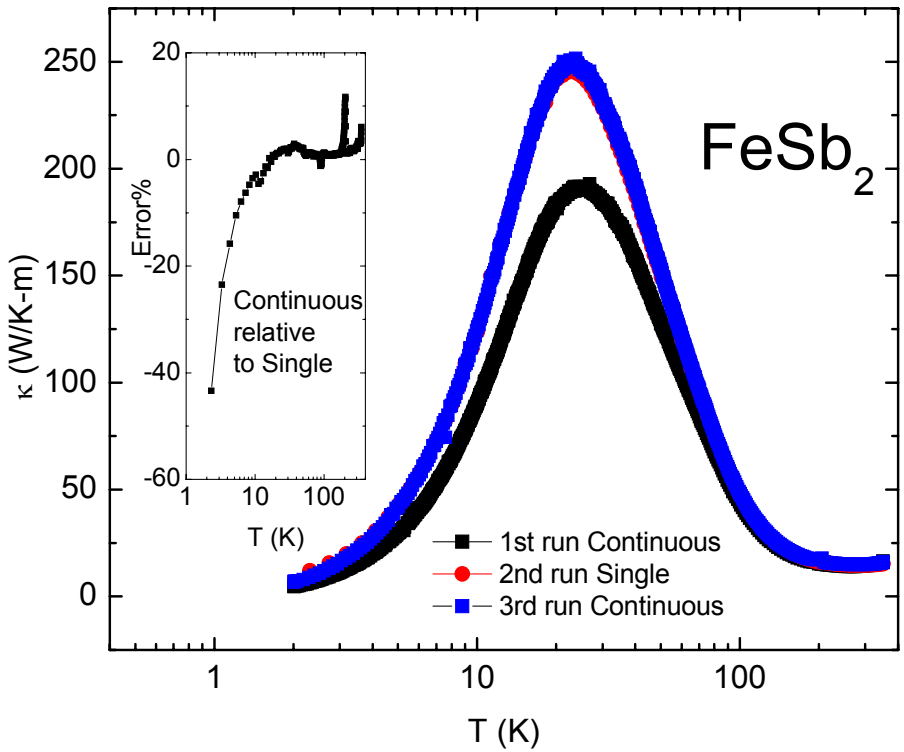

Thermoelectric Materials: $FeSb_2$

europhysicsnews

2008: 40th Anniversary of the EPS
Ethics of nanotechnology or… nanoethics?
Forum Physics and Society I & II
"On the way we conference"
Global mapping of greenhouse gases and air pollutants

38/6
2007
Volume 38 · numb
Institutional subscri
99 euros per year

Colossal Seebeck coefficient in semiconducting $FeSb_2$

Rare-earth, actinide or transition-metal containing correlated semiconductors are characterised by a small hybridisation gap at the Fermi level from mixing of a broad conduction band with a narrow *d*- or *f*-band. Such materials are expected to have large absolute values of the Seebeck coefficient, $S=V/DT$, where V is the voltage difference due to charge carrier diffusion from a hot to a cold region of a material with a temperature difference T.

The figure shows the electrical resistivity (ρ) of single crystalline $FeSb_2$. $\rho(T)$ is semi-conducting and decreases with increasing temperature with a 'shoulder' in the temperature range from 10 K to 30 K. The Seebeck coefficient (S) drops to a sample dependent local minimum which in one sample reaches the record low value of -45000 mVK^{-1}. A plausible interpretation of these properties involves excitations of charge carriers across a very narrow band-gap formed by Fe *3d* states weakly hybridised with Sb *5p* states whose coherence starts to deteriorate when the temperature increases above 10 K. The thermoelectric conversion efficiency increases monotonically with $ZT=(S^2 \cdot r \cdot \rho^{-1}/\kappa)\cdot T$, κ being the thermal conductivity. Materials with $ZT>1$ are considered useful for thermoelectric cooling or power applications. The thermoelectric power factor $PF=S^2 \cdot r \cdot \rho^{-1}$, an important part of ZT, is also shown in the figure. At 12 K the power factor reaches a record high value of ~2300 $mWK^{-2}cm^{-1}$, however a large κ reduces ZT to 0.005. Nonetheless, if κ is reduced to ~3 $Wm^{-1}K^{-1}$, as observed in *e.g.* thin films, ZT~1 can be obtained thus underlining the potential of $FeSb_2$ as a future solid-state thermoelectric cooling device. ■

Anders Bentien, Simon Johnsen, Georg Kent Hellerup Madsen, Bo Brummerstedt Iversen and Frank Steglich, "Colossal Seebeck coefficient in strongly correlated semiconductor $FeSb_2$", *Eur. Phys. Lett.* 80, 17008 (2007)

epl A Letters Journal Exploring the Frontiers of Physics

October 2007

EPL, 80 (2007) 17008
doi: 10.1209/0295-5075/80/17008

www.epljournal.org

Colossal Seebeck coefficient in strongly correlated semiconductor $FeSb_2$

A. Bentien[1(a)], S. Johnsen[2], G. K. H. Madsen[2], B. B. Iversen[2] and F. Steglich[1]

[1] *Max Planck Institute for Chemical Physics of Solids - Nöthnitzer Straße 40, 01187 Dresden, Germany*
[2] *Department of Chemistry, University of Aarhus - Langelandsgade 140, 8000 Århus C, Denmark*

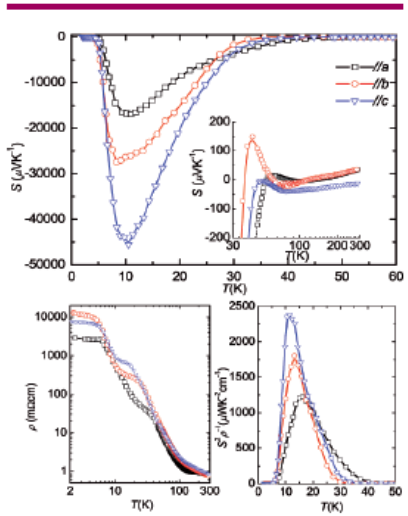

▲ Electrical transport properties as function of temperature along different crystallographic directions on different single crystalline $FeSb_2$ samples.

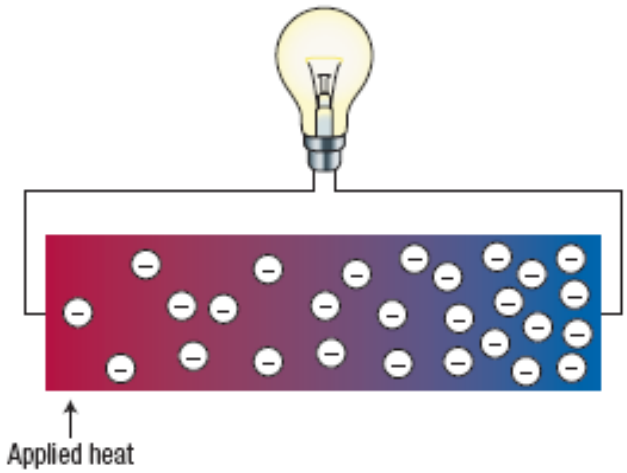

Figure 1 Schematic drawing of a thermoelectric device. The application of a temperature gradient generates a voltage that can be used to power electrical devices.

Thermoelectric Materials

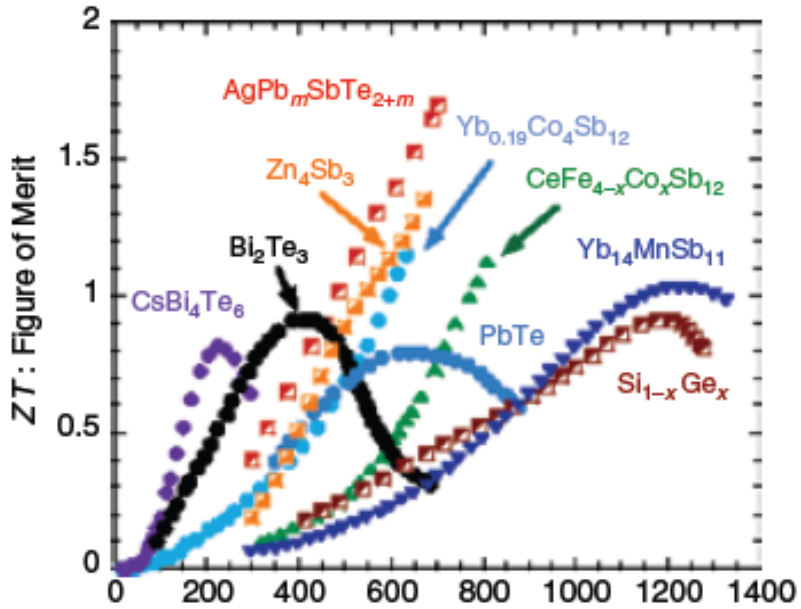

PGEC concept

Wiedemann Franz law $\kappa = L\sigma T$

MRS Bulletin 33, 366 (2008)
Nature Materials 7, 105 (2008)

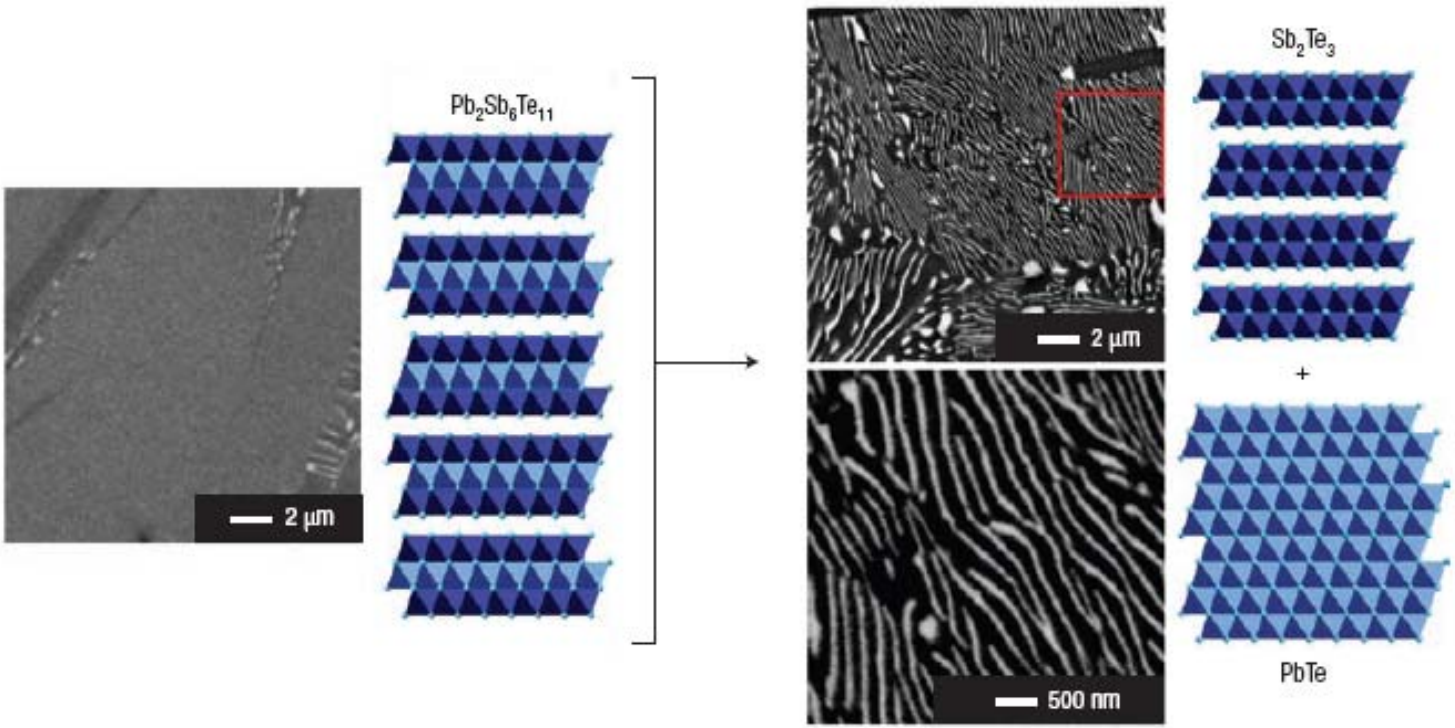

$$ZT = \frac{S^2 T}{\rho(\kappa_{el} + \kappa_{ph})}$$

Thermoelectric Devices

Seebeck
$V = S\Delta T$

	Wavelenth	Spectrum	%
Photovoltaic	~200–800nm	UV & visible light	58
Thermoelectric	~800–3000nm	IR	42

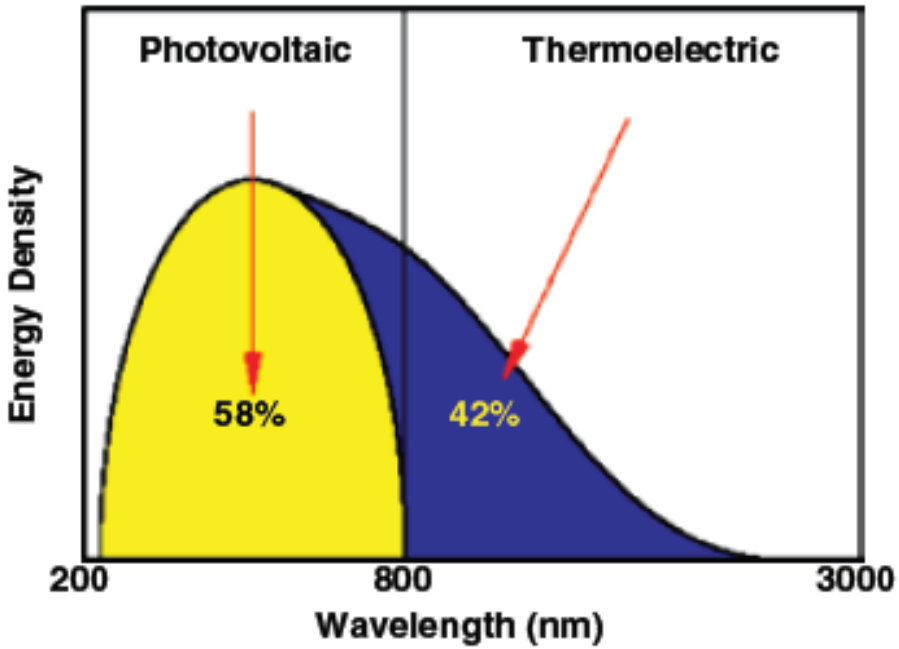

Figure 2. Sun radiates energy as a 6000 K blackbody radiator with part of the energy in the ultraviolet (UV) spectrum and part in the infrared (IR) spectrum.

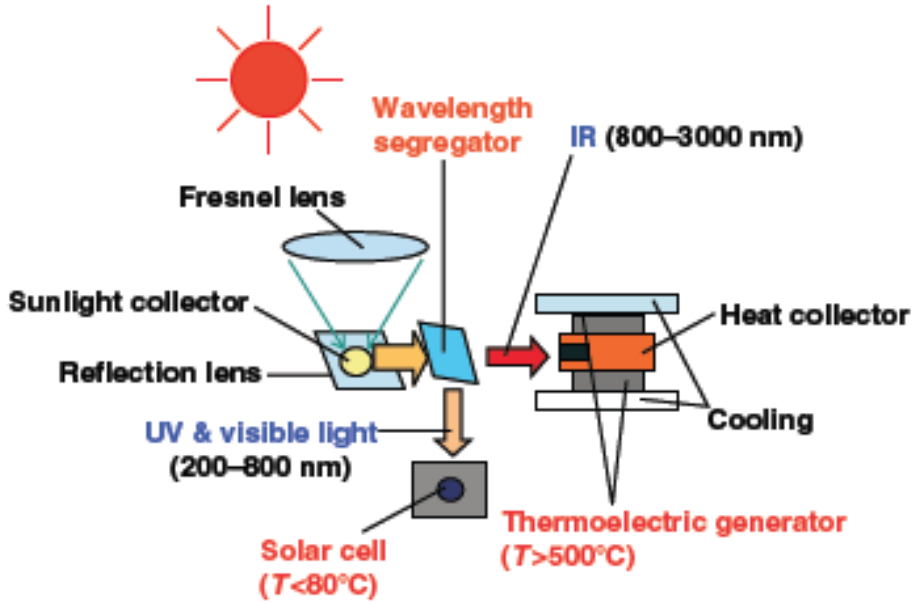

Figure 3. After the solar energy is concentrated, it can be converted into electricity through both photovoltaics (UV spectrum) and thermoelectrics (IR spectrum).

MRS Bulletin 33, 366 (2008)
Nature Materials 7, 105 (2008)